IFN-γ–dependent interactions between tissue-intrinsic γδ T cells and tissue-infiltrating CD8 T cells limit allergic contact dermatitis

Miguel Muñoz-Ruiz, PhD,[a,b,c] Miriam Llorian, PhD,[d] Rocco D'Antuono, MS,[e] Anna Pavlova, MS,[f] Anna Maria Mavrigiannaki, MS,[a] Duncan McKenzie, PhD,[a,b] Bethania García-Cassani, PhD,[g] Maria Luisa Iannitto, PhD,[b] Yin Wu, MD, PhD,[a,b,h] Robin Dart, MD, PhD,[a,b] Daniel Davies, MD,[a,b] Mariam Jamal-Hanjani, MD, PhD,[i] Anett Jandke, PhD,[a,b] Dmitry S. Ushakov, PhD,[a,b,j] and Adrian C. Hayday, PhD[a,b,h] *London, United Kingdom; Madrid, Spain; and Erlangen and Greifswald-Insel Riems, Germany*

Background: Elicitation of allergic contact dermatitis (ACD), an inflammatory type 4 hypersensitivity disease, induces skin infiltration by polyclonal effector CD8 αβ T cells and precursors of tissue-resident memory T (T_{RM}) cells. Because T_{RM} have long-term potential to contribute to body-surface immunoprotection and immunopathology, their local regulation needs a fuller understanding.

Objective: We sought to investigate how T_{RM}-cell maturation might be influenced by innate-like T cells pre-existing within many epithelia.

Methods: This study examined $CD8^+$ T_{RM}-cell maturation following hapten-induced ACD in wild-type mice and in strains harboring altered compartments of dendritic intraepidermal γδ T cells (DETCs), a prototypic tissue-intrinsic, innate-like T-cell compartment that reportedly regulates ACD, but by no elucidated mechanism.

Results: In addition to eliciting CD8 T_{RM}, ACD induced DETC activation and an intimate coregulatory association of the 2 cell types. This depended on DETC sensing IFN-γ produced by CD8 cells and involved programmed death-ligand 1 (PD-L1). Thus, in mice lacking DETC or lacking IFN-γ receptor solely on γδ cells, ACD-elicited CD8 T cells showed enhanced proliferative and effector potentials and reduced motility, collectively associated with exaggerated ACD pathology. Comparable dysregulation was elicited by PD-L1 blockade *in vitro*, and IFN-γ–regulated PD-L1 expression was a trait of human skin-homing and intraepithelial γδ T cells.

Conclusions: The size and quality of the tissue-infiltrating CD8 T-cell response during ACD can be profoundly regulated by local innate-like T cells responding to IFN-γ and involving PD-L1. Thus, interindividual and tissue-specific variations in tissue-intrinsic lymphocytes may influence responses to allergens and other challenges and may underpin inflammatory pathologies such as those repeatedly observed in γδ T-cell–deficient settings. (J Allergy Clin Immunol 2023;152:1520-40.)

Key words: *Tissue-intrinsic innate-like lymphocytes, tissue-resident memory T cells, γδ T cells, tissue immuno-ecology, IFN-γ, PD-L1*

Although immunological memory is a defining tenet of adaptive immunity, the factors that regulate the phenotypes and locations of different memory lymphocyte compartments remain largely unknown.[1,2] In this regard, there is ever-increasing acceptance that important memory responses are launched by tissue-resident memory T (T_{RM}) cells in peripheral extralymphoid sites, such as the lungs, gut, or skin. Those cells seemingly mature under the influence of local cues from precursors evoked in local lymph nodes concurrent with the initial effector response to primary challenge. However, anatomical space constraints emphasize the importance of limiting the scope of the tissue-infiltrating effector T-cell response and its maturation toward a durable T_{RM}-cell compartment.[1,2]

Among possible local regulatory mechanisms, it is important to note that effector T cells and T_{RM}-cell precursors recruited to tissues frequently enter environments already occupied by other immune cell types, including tissue-intrinsic T cells that become associated with a tissue developmentally, rather than following systemic priming. Thus, effector CD8 T cells and T_{RM}-cell precursors maturing in the murine or human intestinal epithelium will likely encounter large subsets of unconventional intraepithelial lymphocytes expressing either αβ or γδ T-cell receptors (TCRs). Nonetheless, although T_{RM}-cell maturation in the murine epidermis has been well-studied, little attention has been paid to how it may be influenced by the presence of intraepidermal γδ T cells, known as dendritic epidermal T cells (DETCs), which express a canonical $Vγ5Vδ1^+$ TCR, and which compose a large, highly organized intraepithelial compartment that develops exclusively in the fetus, that displays lifelong self-renewal, and that contributes to epidermal homeostasis.[3-7]

In fact, there exist clear examples of local γδ T-cell regulation of epidermal αβ T cells. For example, DETCs limit cutaneous graft-

From [a]the Immunosurveillance Laboratory, [d]the Bioinformatics and Biostatistics science technology platform (STP), [e]the Light Microscopy STP, and [g]the Development and Homeostasis of the Nervous System Laboratory, The Francis Crick Institute, London; [b]the Peter Gorer Department of Immunobiology and [h]the Centre for Inflammation Biology and Cancer Immunology, King's College London, London; [c]the Department of Immunology, Ophthalmology and Ear, Nose and Throat, Complutense University School of Medicine and 12 de Octubre Health Research Institute, Madrid; [f]the Department of Biology, Division of Genetics, Nikolaus-Fiebiger-Center for Molecular Medicine, Erlangen; [i]the Cancer Research UK Lung Cancer Centre of Excellence, University College London Cancer Institute, London; and [j]the Institute of Molecular Virology and Cell Biology, Friedrich-Loeffler-Institut, Federal Research Institute for Animal Health, Greifswald-Insel Riems.

Received for publication January 16, 2023; revised June 27, 2023; accepted for publication July 21, 2023.

Available online August 8, 2023.

Corresponding author: Adrian C. Hayday, PhD, King's College London School of Medicine, 2nd Floor Borough Wing, London, SE1 9RT, UK; or The Francis Crick Institute, 1 Midland Rd, London, NW1 1AT, UK. E-mail: adrian.hayday@kcl.ac.uk or adrian.hayday@crick.ac.uk.

The CrossMark symbol notifies online readers when updates have been made to the article such as errata or minor corrections

0091-6749

© 2023 The Authors. Published by Elsevier Inc. on behalf of the American Academy of Allergy, Asthma & Immunology. This is an open access article under the CC BY license (http://creativecommons.org/licenses/by/4.0/).

https://doi.org/10.1016/j.jaci.2023.07.015

Abbreviations used

ACD: Allergic contact dermatitis
CLA: Cutaneous lymphocyte antigen
DETC: Dendritic epidermal T cell
DNFB: 1-Fluoro-2,4-dinitrobenzene
FACS: Fluorescence-activated cell sorting
FVB: Friend leukemia virus B
GEO: Gene Expression Omnibus
GFP: Green fluorescent protein
LC: Langerhans cell
PCA: Principal component analysis
PD-L1: Programmed death-ligand 1
RNA-seq: RNA-sequencing
scRNA-seq: Single-cell RNA-seq
Tac: FVB/NTac
TCR: T-cell receptor
Treg: Regulatory T
T_{RM}: Tissue-resident memory T
t-SNE: t-distributed stochastic neighbor embedding
WT: Wild-type
Yeti: YFP-enhanced transcript for IFN-γ
YFP: Yellow fluorescent protein

versus-host disease induced by inoculation of autoreactive $CD4^+$ αβ T cells, and thereafter exclude subsequent $CD4^+$ T cell inocula from becoming established in the same epidermal site, rendering the mice graft-versus-host disease–resistant.[8] Furthermore, TCRγδ-deficient mice display exaggerated αβ T-cell–dependent allergic contact dermatitis (ACD) responses that could be completely prevented by reconstitution with fetal DETC progenitors.[9] Thus, in these qualitatively distinct settings, local γδ T cells limited the pathogenic potential of infiltrating αβ T cells: nonetheless, potential mechanisms were wholly unexplored.

Of note, mechanistic insights into how γδ-DETCs regulate T_{RM} cells might give clues of general importance, given that many anatomical sites ranging from the gut to the testicles display inflammatory pathologies in γδ T-cell–deficient mice.[10-12] Moreover, the study of DETCs has repeatedly provided fundamental insights into body surface immunology, applicable to species, including humans, that lack a formal DETC-equivalent, but that harbor many other tissue-associated T-cell compartments.[5,13-17] Those insights reflect the fact that the murine epidermis is vitally important for barrier maintenance, is exposed to infections and other insults, and, by being dominated at steady-state by a single tissue-intrinsic lymphocyte compartment (DETC), offers a simplified experimentally tractable system to assess the biology of tissue-intrinsic T cells.

Thus, to better understand how tissue-intrinsic T cells might interact with tissue-infiltrating CD8 T cells, we have returned to chemically induced ACD, a prevalent T-cell–dependent pathology of humans that is commonly modeled in mice;[9,18-20] that elicits a local CD8 T-cell response, including a local T_{RM}-cell compartment that contributes to immunopathology on chemical re-exposure;[21] and that is regulated by local γδ T cells, albeit by unknown mechanism(s).[9] Here we show that several parameters of the elicited murine polyclonal CD8 T-cell compartment are profoundly influenced by local γδ T cells. As one component of this crosstalk, we found that elicited CD8 T cells generated IFN-γ, which induced programmed death-ligand 1 (PD-L1) on local γδ T cells, and that the 2 cell types intimately interacted as T_{RM}-cell maturation was occurring in the early stages of ACD. This interaction imposed overt constraint on the local CD8 T cells, akin to checkpoint blockade. Indeed removing either DETCs, or the *Ifngr* gene from DETCs significantly dysregulated the proliferative, effector, and motility traits of the elicited CD8 T cells, outcomes that were phenocopied *in vitro* by anti–PD-L1. Additionally, CD8 T cells in the absence of DETC-mediated regulation showed reduced expression of CD5, a sentinel of T cells with reduced TCR affinity for antigen.[22-24] Collectively these changes were associated with exaggerated inflammation, consistent with long-standing findings.[9] Thus, our finding argues that ACD should be viewed as an aggregate response of infiltrating CD8 T cells and neighboring tissue-intrinsic lymphocytes, with the 2 cell types jointly composing a local, cross-regulating immunological ecosystem. While the details of such anatomical site-specific regulation may not be precisely conserved in every tissue or species, the underlying principles of local immunological ecosystems may well be and consistent with which we offer anatomically distinct examples of human γδ cells expressing PD-L1 upregulated by IFN-γ, as is the case in the mouse.

METHODS

Resource availability

Lead contact. Further information and requests for resources and reagents should be directed to and will be fulfilled by the lead contact, A.C.H.).

Materials availability. Mouse lines generated in this study will be maintained in the lead author's (A.C.H.'s) current institute's animal house and/or stored locally as frozen embryos and can be made available on request.

Data and code availability. The RNA-sequencing (RNA-seq) datasets reported in this paper can be found at Gene Expression Omnibus (GEO): GSE164023 (GSE164022). The single-cell RNA-seq (scRNA-seq) datasets reported in this paper can be found at GEO: GSE164023 (GSE164021). The RNA-seq data set reported in Fig 4, *D* has been submitted: GEO: GSE160477. Flow cytometry data (from the TRACERx study) used or analyzed during this study are available through the CRUK and UCL Cancer Trials Centre (ctc.tracerx@ucl.ac.uk) for academic non-commercial research purposes. Access will be granted upon review of a project proposal, which will be evaluated by a TRACERx data access committee, and entering into an appropriate data access agreement, subject to any applicable ethical approvals.

Experimental model and subject details

Mice. Adult male mice were used at 4-20 weeks of age. All mice were bred at the Francis Crick Institute (London, United Kingdom). C57BL/6J background: C57BL/6J.WT, $TCR\delta^{-/-}$, $TCR\beta^{-/-}$, $TCR\delta^{-/-}TCR\beta^{-/-}$, $Ifngr2^{fl/fl}$,[25] yellow fluorescent protein (YFP)-enhanced transcript for IFN-γ (Yeti),[26] $Nur77^{GFPCre}$,[27] $Ifngr1^{-/-}$,[28] and $Tcrd^{Cre}$.[29] $Ifngr2^{fl/fl}$ mice were kindly provided by Jean Langhorne (Francis Crick Institute). Friend leukemia virus B (FVB) background: FVB.WT, $FVB.\delta^{-/-}$, $FVB.V\gamma5^{-/-}V\delta1^{-/-}$, $FVB.\beta^{-/-}$, $FVB.\beta^{-/-}\delta^{-/-}$, $FVB.cxcr6^{tm1Litt}$, and FVB/NTac (Tac) mice carrying a mutation in the *Skint1* gene were from Taconic farms (Taconic

TABLE I. Key resources

Reagent or resource	Source	Identifier
Antibodies		
Brilliant violet 605 anti-mouse CD8a (53-6.7)	BioLegend	Cat# 100744, RRID: AB_2562609
PE anti-mouse CD5 (53-7.3)	BD Biosciences	Cat# 553022, RRID: AB_394560
Brilliant violet 605 anti-mouse CD5 (53-7.3)	BD Biosciences	Cat# 563194, RRID: AB_2738061
FITC anti-mouse Ly-6A/E (Sca-1) (D7)	eBioscience	Cat# 11-5981-82, RRID: AB_465333
APC anti-mouse CD103 (2E7)	BioLegend	Cat# 121413, RRID: AB_1227503
PE anti-mouse CD103 (2E8)	BioLegend	Cat# 121406, RRID: AB_1133989
PE/Cy7 anti-mouse CD8a (53-6.7)	BioLegend	Cat# 100722, RRID: AB_312761
Pacific blue anti-mouse CD8a (53-6.7)	BioLegend	Cat# 100725, RRID: AB_493425
PE/Cy7 anti-mouse CD69 (H1.2F3)	BioLegend	Cat# 104512, RRID: AB_493564
APC/Cy7 anti-mouse CD69 (H1.2F3)	BioLegend	Cat# 104526, RRID: AB_10679041
PE/Cy7 anti-mouse/human CD44 (IM7)	BioLegend	Cat# 103030, RRID: AB_830787
PerCP/Cy5.5 anti-mouse CD45 (30-F11)	BioLegend	Cat# 103132, RRID: AB_893340
APC/Cy7 anti-mouse CD45 (30-F11)	BioLegend	Cat# 103116, RRID: AB_312981
FITC anti-mouse TCR-γδ (GL3)	BioLegend	Cat# 118106, RRID: AB_313830
Brilliant violet 421 anti-mouse TCR-γδ (GL3)	BioLegend	Cat# 118119, RRID: AB_10896753
Brilliant violet 421anti-mouse TCR-β (H-57)	BioLegend	Cat# 109230, RRID: AB_2562562
APC anti-mouse TCR-β (H-57)	BioLegend	Cat# 109212, RRID: AB_313435
Brilliant violet 605 anti-human/mouse/rat CD278 (ICOS) (C398.4A)	BioLegend	Cat# 313538, RRID: AB_2687079
Alexa Fluor 647 anti-human/mouse/rat CD278 (ICOS) (C398.4A)	BioLegend	Cat# 313516, RRID: AB_2122582
APC anti-mouse CD314 (NKG2D) (CX5)	BioLegend	Cat# 130212, RRID: AB_1236372
PE anti-mouse CD314 (NKG2D) (CX5)	BioLegend	Cat# 130207, RRID: AB_1227713
FITC anti-mouse CD314 (NKG2D) (C7)	BioLegend	Cat# 115711, RRID: AB_2133291
PE/Cy7 anti-mouse CD159a (NKG2AB6) (16A11)	BioLegend	Cat# 142809, RRID: AB_2728160
APC/Cy7 anti-mouse CD3ε (2C11)	BioLegend	Cat# 100330, RRID: AB_1877170
Brilliant violet 605 anti-mouse CD119 (IFN-γ Rα) (GR20)	BD Biosciences	Cat# 745111, RRID: AB_2742716
PE IFN-γR β chain antibody	Miltenyi Biotec	Cat# 130-105-671, RRID: AB_2652252
Brilliant violet 605 anti-mouse CD366 (Tim-3) (RMT3-23)	BioLegend	Cat# 119721, RRID: AB_2616907
PE anti-mouse CD254 (TRANCE, RANKL) (IK22/5)	BioLegend	Cat# 510005, RRID: AB_315553
PE anti-mouse CD137 antibody (17B5)	BioLegend	Cat# 106106, RRID: AB_2287565
FITC anti-mouse CD279 (PD-1) (29F.1A12)	BioLegend	Cat# 135214, RRID: AB_10680238
Brilliant violet 421 anti-mouse CD274 (B7-H1, PD-L1) (10F.9G2)	BioLegend	Cat# 124315, RRID: AB_10897097
PE anti-mouse TIGIT mAb (GIGD7)	eBioscience	Cat# 12-9501-82, RRID: AB_11042152
Purified anti-mouse CD274 (B7-H1, PD-L1) (10F.9G2)	BioLegend	Cat# 124302, RRID: AB_961228
Purified rat IgG_{2b}, κ isotype control (RTK4530)	BioLegend	Cat# 400601, RRID: AB_326545
TCR-β mAb (H57-597), functional grade	eBioscience	Cat# 16-5961-82, RRID: AB_469169
PE anti-human/mouse CLA antibody	BioLegend	Cat# 321311, RRID: AB_2565588
APC anti-human CD274 (B7-H1, PD-L1) antibody	BioLegend	Cat# 393609, RRID: AB_2749926
TCR Vδ1 antibody, anti-human, REAfinity	Miltenyi Biotec	Cat# 130-120-442, RRID: AB_AB_2752100
FITC anti-human TCR Vδ2 antibody	BioLegend	Cat# 331405, RRID: AB_1089231
Chemicals, peptides, and recombinant proteins		
FBS, heat inactivated	Gibco (Thermo Fisher Scientific)	Cat# 10270106
Penicillin-streptomycin	Sigma-Aldrich	Cat# P4333
RPMI 1640	Gibco	Cat# 21875-091
LIVE/DEAD Fixable Blue Dead Cell Stain Kit	Thermo Fisher Scientific	Cat# L34962
Hoechst 33342	Thermo Fisher Scientific	Cat# H3570
Olive oil	Sigma-Aldrich	Cat# 75343
Acetone	Thermo Fisher Scientific	Cat#
DNFB	Sigma-Aldrich	Cat# D1529
Red Blood Cell Lysing Buffer Hybri-Max	Sigma-Aldrich	Cat# R7757
4-OH tamoxifen	Sigma-Aldrich	Cat# H7904
Ammonium thiocyanate	Sigma-Aldrich	Cat# A7149
Trypsin from bovine pancreas	Sigma-Aldrich	Cat# T1005
DNase I from bovine pancreas	Sigma-Aldrich	Cat# 11284932001
Trypsin/EDTA solution	Gibco	Cat# 25200-056
HBSS	Thermo Fisher Scientific	Cat# 14175095
Collagenase type IV	Worthington	LS004188
DNAse I	Sigma-Aldrich	Cat# D5025-15
BSA	Sigma-Aldrich	Cat# A4503
rTGFb	PeproTech	Cat# 100-21
Recombinant mouse IL15	ImmunoTools	Cat# 12340155

(Continued)

TABLE I. *(Continued)*

Reagent or resource	Source	Identifier
Matrigel	Corning	Cat# 734-0270
Critical commercial assays		
CD8a+ T-Cell Isolation Kit, mouse	Miltenyi Biotec	Cat# 130-104-075
Deposited data		
RNA-seq data	This paper	GEO: GSE63473
scRNA-seq data	This paper	GEO: GSE164023
Experimental models: organisms/strains		
Mouse: WT: C57BL/6J	Jackson Laboratory	Cat# JAX:000664; RRID: IMSR_JAX:000664
Mouse: C57BL/6-Tg(Nr4a1-EGFP/cre)820Khog/J	Jackson Laboratory	Cat# JAX:016617, RRID: IMSR_JAX:016617
Mouse: B6.129P2-Tcrdtm1Mom/J	Jackson Laboratory	Cat# JAX:002120, RRID: IMSR_JAX:002120
Mouse: B6.129P2-Tcrbtm1Mom/J	Jackson Laboratory	Cat# JAX:002118, RRID: IMSR_JAX:002118
Mouse: B6.129P2-Tcrbtm1Mom Tcrdtm1Mom/J	Jackson Laboratory	Cat# JAX:002122, RRID: IMSR_JAX:002122
Mouse: Yellow fluorescent protein (YFP)-enhanced transcript for IFN-γ (Yeti)	Francis Crick Institute	Stetson et al[26]
Mouse: B6.129S7-Ifngr1tm1Agt/J	Jackson Laboratory	Cat# JAX:003288, RRID: IMSR_JAX:003288
Mouse: IFN-γR2 floxed	Francis Crick Institute	Kok et al[25]
Mouse: B6.129S-Tcrdtm1.1(cre/ERT2)Zhu/J	Jackson Laboratory	Cat# JAX:031679, RRID: IMSR_JAX:031679
Mouse: FVB/NJ (FVB.WT)	Francis Crick Institute	Cat# JAX:001800, RRID: IMSR_JAX:001800
Mouse: FVB.$\delta^{-/-}$	Francis Crick Institute	
Mouse: FVB/NTac (FVB.Tac)	Francis Crick Institute	
Mouse: FVB.V$\gamma5^{-/-}$;V$\delta1^{-/-}$	Francis Crick Institute	
Mouse: FVB.$\beta^{-/-}$	Francis Crick Institute	
Mouse: FVB.$\beta^{-/-}\delta^{-/-}$	Francis Crick Institute	
Mouse: FVB.Cxcr6tm1Litt	Francis Crick Institute	
Mouse: FVB/N.R26 mTmg	Francis Crick Institute	
Software and algorithms		
ImageJ	Developer: Wayne Rasband (NIH)	https://imagej.nih.gov/ij/, RRID: SCR_003070
GraphPad Prism version 8.0.2	GraphPad Inc	RRID: SCR_002798
FlowJo version 10	BD	RRID: SCR_008520

APC, Antigen-presenting cell; *Cy*, cyanine; *FITC*, fluorescein isothiocyanate; *PE*, phycoerythrin; *PerCP*, peridinin chlorophyll; *TRANCE*, TNF superfamily member 11 (TNFSF11).*

*eBioscience: Thermo Fisher Scientific (UK); Worthington: Worthington Biochemical (US); Peprotech: Rocky Hill, NJ; ImmunoTools: ImmunoTools GmbH, Gladiolenweg, Germany; Corning: Corning Inc (US); Jackson Laboratory: The Jackson Laboratory (US).

Biosciences, Germantown, NY) (Table I). Mice were kept in filter-topped cages with sterilized food and water *ad libitum* and autoclaved corncob bedding that was changed at least once weekly. All experiments were performed according to the UK animal protection laws.

Humans. *Gut.* Human endoscopy biopsies were obtained from macroscopically healthy mucosa from the ascending colon of adult patients undergoing diagnostic colonoscopy after informed consent was obtained and in compliance with ethical approval (16/LO/0642) from the National Health Service Health Research Authority (London—Fulham Research Ethics Committee).

Lung. All clinical samples used were collected from patients recruited to the lung TRACERx (Tracking Non-small Cell Lung Cancer Evolution Through Therapy) study (approved by an independent Research Ethics Committee, National Research Ethics Service Committee London, REC:13/LO/1546; https://clinicaltrials.gov/ct2/show/NCT01888601). All participants provided informed consent before taking part. Participants were not compensated.

PBMC. PBMCs were isolated from cone blood samples provided by the NHS Blood and Transplant service (London, UK) by Ficoll gradient centrifugation.

Experimental protocols

Contact dermatitis. To induce ACD, mice were sensitized on day 0 by epicutaneous application to razor-shaved abdominal skin (with Wella clippers and wecprep blades from Pilling [Teleflex Inc, Morrisville, NC]) of 40 μL of 0.5% 1-fluoro-2,4-dinitrobenzene (DNFB) in a mixture of acetone–olive oil (3:1). On day 6, mice were challenged (first challenge) by applying 20 μL of 0.25% DNFB in acetone–olive oil at the back skin or ear. In some cases, mice were rechallenged 21 days later (second challenge) (Table I). In collaboration with Making STP at the Francis Crick Institute, a device was developed to ensure the area of application was consistent across the experiments (50 mm^2).

Adoptive transfers. For adoptive transfer, $CD8^+$ T cells were purified from spleen and lymph nodes by $CD8\alpha^+$ T Cell Isolation Kit, mouse (Miltenyi Biotec, Auburn, Calif) according to the manufacturer's instructions and 1×10^6 wild-type (WT) $CD8^+$ T cells were intravenously transferred into T-cell–deficient animals denoted in the text. The following day, mice were sensitized and challenged.

Topical tamoxifen treatment. 4-Hydroxytamoxifen (4-OH tamoxifen) (H7904-25MG; Sigma-Aldrich, St Louis, Mo) was dissolved in 99.5% acetone following incubation at 37°C for

5-10 minutes with occasional vortexing. A final concentration of 12 mg/mL was administered to mice for 5 consecutive days by topical application (20 μL/ear).

CD8 *in vitro* culture. Total $CD8^+$ T cells were isolated ($CD8\alpha^+$ T Cell Isolation Kit, mouse; Miltenyi Biotec) from spleens of sensitized mice 5 days after DNFB application and transferred into 96-well plates with cytokines and/or antibodies described in the text. Two days after, $CD8^+$ T cells were analyzed phenotypically by flow cytometry.

Isolation of primary DETC lines (short-term DETC). Primary DETCs were isolated and grown as previously described.[16] After approximately 1 month, cells were assessed for purity by flow cytometry. Cell lines with ≥85% DETCs were used for coculture experiments.

T_{RM}-DETC coculture assays. Primary DETC lines were isolated as described previously. T_{RM}-cell were sorted (see FACS sorting) 21 days after the second challenge and added to primary DETC cultures in a 96-well plate at a concentration of 4×10^4 cells/type of cell. All cells were collected 72 hours later.

Human culture assays. *Gut.* Primary gut lymphocytes were obtained using an adaptation of the method of Kupper and Clarke.[30] Cellfoam matrices (9 mm × 9 mm × 1.5 mm; Cytomatrix PTY Ltd, Hawthorn East, Victoria, Australia), were autoclaved and incubated in 100 mg/mL rat tail collagen I (BD Biosciences, San Jose, Calif) in PBS for 30 minutes at 37°C, and washed twice in PBS. In compliance with local ethical approval, endoscopic biopsies were taken from the ascending colon of donors. Biopsies were washed for 20 minutes in 5 mL wash medium (RPMI 1640 10% FCS, β-mercaptoethanol, penicillin [500 U/mL], streptomycin [500 μg/mL], metronidazole [5 μg/mL; Pharmacy department, Guy's Hospital, London, United Kingdom], gentamicin [100 μg/mL; Sigma-Aldrich], and amphotericin 12.5 μg/mL [Thermo Fisher Scientific, Waltham, Mass]). One endoscopic biopsy was placed on top of each matrix, which was inverted, and pressure applied, to crush the biopsy into the matrix. The matrices were placed into a 24-well plate (1 per well) and covered with 1 mL RPMI 1640 (supplemented with complete media: 10% FCS, β-mercaptoethanol, penicillin [100 U/mL], streptomycin [100 μg/mL], metronidazole [1 μg/mL], gentamicin [20 μg/mL], amphotericin [2.5 μg/mL]) or complete media supplemented with 0.5 μg/mL recombinant IFN-γ [BioLegend, San Diego, Calif]. Cells were harvested after 24-hour culture and residual biopsy and empty wells were washed with PBS 0.02 mmol/L HEPES. The cell suspension was passed through a 70-μm nylon cell strainer, centrifuged at 400*g* for 5 minutes. Cells were subsequently analyzed by flow cytometry.

Lung. Tissue specimens were reviewed by a lung pathologist as previously described.[31] Of note, non-tumor (NT) tissues were taken as far away as possible from tumors at primary surgery and H&E sections examined afterwards by a trained histopathologist to ensure that samples were fully tumor-free. Fresh NT tissues were finely minced with sterile scalpels and dissociated in type 1 collagenase (10 U/mL, Thermo Fisher Scientific) and DNase I (75 μg/mL, Roche) on a gentleMACS (Miltenyi Biotech) for 60 min at 37 °C. Digested material was passed through a 0.07 mm cell filter before tumor-infiltrating lymphocyte (TIL) enrichment by Ficoll-paque gradient centrifugation (GE Healthcare). Isolated TILs were frozen in 10% dimethylsulfoxide (DMSO)/fetal calf serum (FCS) and stored in liquid nitrogen until analysis.

Flow cytometry. To analyze epidermal T-cell populations, separate epidermal cell suspensions were prepared as described[32] from ears or back skin of individual animals. When back skin was analyzed, always the same amount of skin (equivalent to 962 mm^2) was digested. After overnight culture to allow re-expression of trypsin-sensitive epitopes, epidermal cells were blocked with normal hamster IgG plus anti-FcR (2.4G2), and stained with anti-CD8α (53-6.7), anti-CD5 (53-7.3), anti-Ly-6A/E (Sca-1) (D7), anti-CD103 (2E7), anti-CD69 (H1.2F3), anti-CD44 (IM7), anti-CD45 (30-F11), anti-TCR γδ(GL3), anti-TCR β(H-57), anti-CD278 (ICOS) (C398.4A), anti-CD314 (NKG2D [KLRK1]) (CX5), anti-CD314 (NKG2D) (C7), anti-CD159a (16A11), anti-CD3 ε (2C11), anti-CD119 (GR20), anti-CD366 (RMT3-23), anti-CD254 (IK22/5), anti-CD137 antibody (17B5), anti-CD279 (PD-1) (29F.1A12), anti-CD274 (B7-H1, PD-L1) (10F.9G2), and anti-TIGIT (GIGD7) (Table I). Isotype-matched control antibodies were used at the same concentrations as test antibodies. Analysis was performed with a LSRFortessa (BD Biosciences) with electronic gates set on live cells by a combination of forward and side light scatter and propidium iodide exclusion. A minimum of 100 live events was collected per sample and data were analyzed with FlowJo software (BD, Franklin Lakes, NJ).

FACS sorting for bulk RNA-seq and scRNA-seq. To isolate epidermal T-cell populations, separated epidermal cell suspensions were prepared as described from back skin of individual animals,[32] incubated with mAbs for 30 minutes at 4°C in fluorescence-activated cell sorting (FACS) buffer (2% FBS in PBS, pH 7.4, stabilized with 0.09% sodium azide), then washed twice in FACS buffer. Viable $CD45^+CD103^+TCR\beta^+CD5^+$ for scRNA-seq and $CD45^+CD3^+TCR\delta^+$ for bulk RNA-seq cells were sorted into PBS buffer + 0.04% BSA and retained on ice. Sorted cells were confirmed to be >85% to 95% pure prior to RNA extraction.

RNA-seq. cDNA was prepared from 10-ng input RNA using the NuGEN Ovation RNA-Seq System (V2; Manchester, United Kingdom), and libraries constructed using the NuGEN Ultralow Library System V2. Both these steps followed the manufacturer's instructions. The resulting libraries were pooled for sequencing on an Illumina HiSeq 2500 platform (San Diego, Calif) with single-ended 75-bp reads. Read adaptor removal and quality trimming was carried out with Trimmomatic (version 0.36; Illumina).[33] Reads were then aligned to the mouse genome, using Ensembl GRCm38, release 86 (Saffron Walden, United Kingdom) as reference. Read alignment and gene level quantification was performed by STAR alignment (v.2.5.2a)[34] together with RSEM package (v.1.2.31).[35] Differential expression analysis was carried out with DESEq2 (v 1.28.0)[36] within R programming environment (R Core Team, Vienna, Austria). Genes are designated as differentially expressed if $P_{adj} < .05$.

scRNA-seq. Samples were prepared using the 10x 3' mRNA-Seq kit version 3.0 (10x Genomics, Pleasanton, Calif). Briefly, cell viability was assessed using an EVE cell counter (NanoEntek, Seoul, Korea) and trypan blue viability stain. Approximately 10,000 cells were loaded into the 10x Genomics Chromium, which was operated according to manufacturer's instructions. Sequencing was carried out on the Illumina HiSeq 4000 with a read configuration recommended by 10x Genomics for the sequencing of these libraries (28-bp read 1, 98-bp read 2, 8-bp index 1). Cell Ranger software (version 2.1.1; 10x Genomics) was used to de-multiplex Illumina BCL (binary base call format) output, create fastq files, and generate single-cell feature counts for each library using mm10-v1.2.0 as

reference. All subsequent analyses were performed in R v.3.5.1 using the Seurat (v 2.3.4) package.[37] Genes were removed if they were expressed in ≤3 cells and cells with <500 genes detected were also removed. Data was integrated following Seurat's vignette. In brief, for each sample the top 1,000 most variable genes were selected for data integration using canonical correlation analysis with 25 dimensions used for dimensional reduction using t-distributed stochastic neighbor embedding (tSNE) and cluster calling. On initial examination of the clusters, we excluded cells that expressed Cd47 >4 times (myeloid cells) and Krt15 >2 times (keratinocytes) prior to integration, and the analysis was repeated with the same parameters using resolution of 0.4 to define clusters. Cluster markers were identified using "FindConservedMarkers" with default parameters. To find genes expressed differentially between WT and Tac mice within each cluster, we used the DESeq2[36] test in "FindMarkers". Gene set enrichment analysis was carried out with the GSEA software (version 2.2.3) from the Broad Institute (Cambridge, Mass). The software compares ranked lists of genes, in this case, differentially expressed genes ranked by the "stat" value obtained from DESeq2 in decreasing order, with gene sets "c2.cp.v7.0.symbols.gmt" and "c5.bp.v7.0.symbols.gmt" downloaded from the Broad Institute.

Quantitative RT-PCR. Epidermis from back skin was separated from dermis as described in the flow cytometry section. To isolate specific epidermal T-cell populations, cell suspensions were prepared as described in the FACS sorting section. Samples were directly frozen in RLT buffer prior to RNA purification with DNAse digest (RNeasy kit; QIAGEN, Venlo, The Netherlands). cDNA was generated using Superscript-II (Invitrogen, Thermo Fisher Scientific) and analyzed using Sybr-green assay (Invitrogen) using a Viaa7 Real-time PCR machine (Applied Biosystems, Thermo Fisher Scientific). cDNA was analyzed for *Skint1* and *Skint2*, and the expression levels of each gene were normalized to cyclophilin.

Confocal microscopy. Ears were separated from their epidermis with 0.5 mol/L ammonium thiocyanate in PBS. The mechanically split ears were floated with their dermal side down in the petri dish and incubated in CO_2 incubator at 37°C for 35 minutes. The epidermis was physically separated from the dermis and it was fixed with cold acetone for 20 minutes. The epidermal sheets were blocked with PBS containing 5% normal goat serum and stained for 1 hour with antibodies at room temperature in PBS containing 5% normal goat serum and 0.5% BSA using TCRδ-BV421 and CD8-FITC antibodies. z-sections were acquired on a Leica SP5 confocal microscope (Leica Microsystems, Deerfield, Ill) using a 10×/1.25 numerical aperture objective and processed and analyzed using Fiji.[38] For quantitative analysis, confocal records were processed to identify cells shown in Fig 4, *B,* using Otsu's automated thresholding and multiresolution segmentation in Definiens Developer XD software (Munich, Germany). Morphological parameter sphericity was calculated as the ratio of cell object border length to its volume, ranging from 0 to 1 with higher values corresponding to more spherical objects.

Confocal microscopy *ex vivo*. Challenged ears of the animals were placed on a #1.5 coverslip to be imaged on a Zeiss Upright LSM880 NLO (Oberkochen, Germany), with a Plan-Apochromat 20×/0.8 numerical aperture objective. Migration of cells was monitored exciting sequentially the sample with 488-nm and 561-nm laser lines, detecting the signal between 510 to 550 nm (green fluorescent protein [GFP] channel) and 580 to 640 nm (tdTomato channel). A volume of 213 mm × 213 mm × 30 mm (*z*-step = 5 mm) was acquired every 30 seconds (time interval), for a total duration of 30 to 60 minutes. Cells were manually tracked using the Manual Tracking plugin available in Fiji[38] and the tracks were analyzed (steps distribution, mean square displacement, and directionality) with custom-made python (Python Software Foundation) scripts.

T_{RM}-cell movement modeling. The simulation includes 2 cell populations, one set to be steady, with no change in XY position (green cells, imitating DETCs), and the other allowed to move (red cells, imitating T_{RM} cells). The behavior of the simulated red cells has been modeled including 2 terms that change the possible movement, compared to randomly generated step size and angles: an "initiation" factor that increases the possible maximum step size, and an "attraction" factor that allows the cell to move with bigger steps toward the nearest cell of the second population if the latter (green cell) happens to be within a proper distance (attraction radius).

Additionally, the model includes terms to simulate potential contacts between the 2 cell populations; in the case of close proximity with a green cell, the red cell direction is generated according to an inhomogeneous angle distribution.

The parameters used to simulate "1" were step_max = 14 μm, activation = 0.99, attraction_radius = 100 μm, attraction_Probability = 0.7; while "2" has been simulated using step_max = 14 μm, activation = 0.2, attraction_radius = 100 μm, attraction_Probability = 0.01.

Normalization and statistical analysis

When indicated in each experiment, every value was divided by the average value of the normal control condition. This process of division allowed us to normalize the data and compare it across different experiments. After normalizing the values, we combined or pooled the data from different experiments.

Groups were compared with Prism software (GraphPad Software, San Diego, Calif) using the 2-tailed unpaired Student *t*-test for comparison of 2 groups or 1-way ANOVA for comparison of 3 groups. Data are presented as each data point and mean or mean ± SD. $P < .05$ was considered significant. The experiments were not randomized, and the investigators were not blinded to allocation during experiments and outcome assessment. No statistical methods were used to predetermine sample size. All experiments were performed at least twice, either with similar results obtained and representative data shown, or with pooled data shown. Graph bars with pooled data from multiple experiments include all experiments performed. Where representative histograms are shown, data reflect ≥2 independent experiments with ≥3 mice per experiment, in which similar results were obtained.

RESULTS

ACD elicits a polyclonal epidermal $CD5^+CD103^+$ CD8 T-cell compartment

Mimicking frequent human exposure to chemical irritants, we employed a well-established system of ACD,[21] in which mice were initially sensitized to DNFB on their abdomen, followed by re-exposure ("challenge") ~6 days later on their back or ear skin (Fig 1, *A*, top panel). During sensitization, naive αβ T cells in the draining lymph nodes undergo antigen-driven clonal expansion

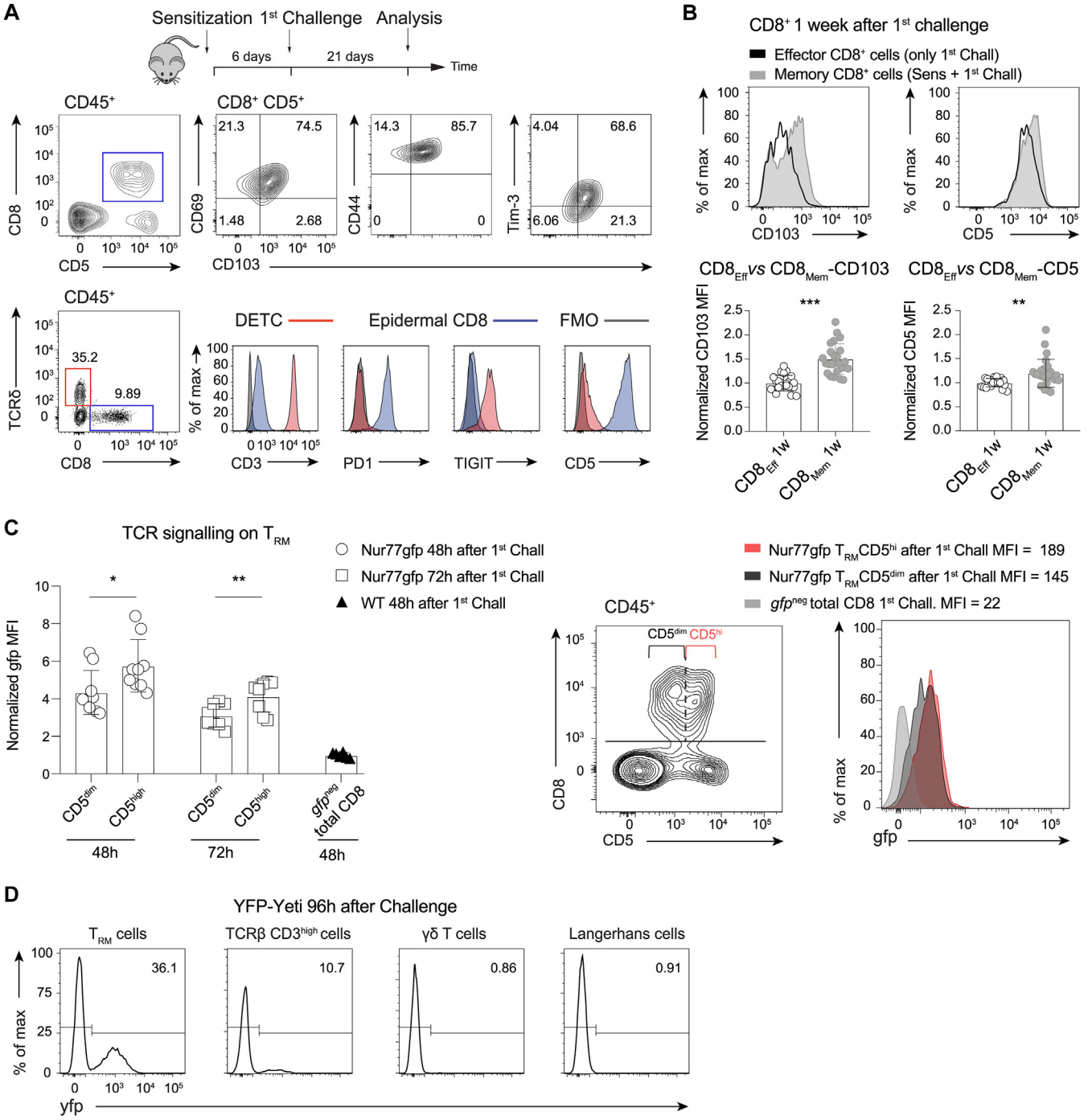

FIG 1. ACD elicits a polyclonal epidermal $CD5^+CD103^+$ CD8+ T-cell compartment. **A,** ACD experimental protocol in WT mice (*upper*); flow cytometry evaluation of $CD8^+CD5^+$ T_{RM} cells (*middle*), and of epidermal $CD103^+CD8^+$ αβ T cells and DETCs (*lower*). **B,** CD103 and CD5 expression on epidermal $CD8^+$ T_{RM} cells and $CD8^+$ T effector cells 1 week after either sensitization (*Sens*) and first challenge or primary antigen challenge alone (*upper*). Bar graphs (*lower*) show normalized mean fluorescent intensity (*MFI*) for CD103 and CD5 1 week after DNFB treatment of ears (n = 24). **C,** (*Left*) Normalized GFP levels on $CD8^+CD5^{high}$ and $CD8^+CD5^{low}$ T cells, 48 and 72 hours after first challenge of $Nur77^{GFP}$ mice (n = 8; data from 3 independent experiments); (*right*) representative flow cytometry of GFP levels on $CD8^+CD5^{high}$ versus $CD8^+CD5^{low}$ T cells, 72 hours after first challenge of $Nur77^{GFP}$ mice ("gfp^{neg} total CD8" denotes signal from nontransgenic WT mice). **D,** Representative analysis of YFP as read-out for IFN-γ measured by flow cytometry 96 hours after first challenge for indicated populations of $CD45^+$ epidermal cells in YFP-Yeti mice. **B, C,** Data are mean ± SD; Student *t*-test. $*P < .05$, $**P < .01$, $***P < .001$. *FMO,* Fluorescence minus one.

and differentiate into effector cells and into cells that are systemic precursors of T_{RM} cells. On allergen challenge, those precursors accumulate at sites of allergen reapplication, initiating a proinflammatory cascade, and developing into mature T_{RM} cells under the influence of local cues.[39] Indeed, applying flow cytometry gating strategies shown (see Fig E1 in this article's Online Repository at www.jacionline.org), we observed increased epidermal αβ T-cell representation in DNFB-sensitized mice following primary and secondary challenges, by comparison to unmanipulated mice (Fig E1 and see Fig E2, *A* in this article's Online Repository at www.jacionline.org), and the infiltrating αβ T cells were primarily $CD8^+$ and were also $CD5^+$ (Fig 1, *A* and Figs E1 and E2, *B*), in clear contrast to $CD5^-$ tissue-intrinsic γδ T cells (Fig E2, *B*).

The epidermal $CD5^+$ $CD8^+$ T cells were mostly $CD103(\alpha E\beta 7)^+$ and $KLRG1^-$ (Fig 1, *A* and Fig E2, *C*), expressed CD69, CD44, and PD1, but only low levels of T-cell immunoglobulin mucin family member 3 (HAVCR2, also known as TIM3) and of TIGIT (Fig 1, *A*), consistent with a phenotype commonly reported for T_{RM} cells.[40,41] Interestingly, the cells mostly displayed very low CD3 expression (Fig 1, *A*), possibly reflecting a protein conformational change since TCRβ staining was not atypically low (Fig E2, *A*). Conversely, $TCR\gamma\delta^+$ DETCs that coinhabit the epidermis displayed essentially the opposite phenotype: $CD3^{hi}$ $PD1^{lo}$ $TIGIT^{hi}$ $CD5^{-/lo}$ (Fig 1, *A* and Fig E2, *B*), demonstrating that whereas the local environment is a major driver of T_{RM}-cell differentiation, it does not impose phenotypic homogeneity on different T-cell subsets.

Further illustrating this point, epidermal $CD8^+$ αβ T cells harvested 1 week after DNFB treatment of mice that had not been previously sensitized were more akin to T-effector cells than to T_{RM} cells, displaying significantly less CD103 upregulation and lower CD5 expression (Fig 1, *B*) (see Methods for how normalization was undertaken). Indeed, in sensitized and challenged mice, significant increases were observed in the percentages of cells that expressed T_{RM}-associated CD103 and CD5, while there was an almost complete loss of cells expressing KLRG1, which is a T-effector cell marker (Fig E2, *C*). Moreover, the levels of expression of CD5 and CD103 were incrementally upregulated between 48 hours and 1 week post challenge, while NKG2D and CD69 expression levels were concurrently reduced by approximately 30% and 50%, respectively (Fig E2, *D*).

With regard to CD5 upregulation, we noted that higher CD5 expression has been reported to mark T_{RM} cells with higher affinity TCRs.[42] Thus, we used *Nur77*^{GFP} mice in which a GFP reporter is expressed from the TCR-regulated promoter of the *Nur77* gene, a gene required for T_{RM}-cell maturation.[43] Hemizygous *Nur77*^{GFP} mice were DNFB-sensitized, challenged 6 days later, and epidermal CD8 T cells were examined 48 and 72 hours post challenge. At both time points, $CD5^{hi}$ versus $CD5^{dim}$ CD8 T cells (gated as in Fig 1, *C*) showed significantly higher GFP levels (≤50% greater) (Fig 1, *C*), indicating that they had experienced stronger TCR-dependent signal transduction. Likewise receptor activator of nuclear factor κB ligand ([RANKL], another TCR-responsive gene),[44] was expressed significantly more strongly (~3-fold) by epidermal $CD5^{hi}$CD8 T cells versus $CD5^{dim}$CD8 T cells (Fig E2, *E*). Conversely, $CD5^{dim}$CD8 and $CD5^{hi}$CD8 T cells expressed comparable levels of CD8 and CD103, neither of which reflects TCR signaling strength (Fig E2, *E*). Thus, in this system of ACD, we consider CD5 levels to be a quantitative index of TCR responsiveness that might therefore be considered a marker of the quality of the elicited polyclonal T_{RM} cells, as is considered further below.

To examine functional potentials of elicited CD8 T cells, we induced ACD in hemizygous YFP-Yeti (enhanced transcript for IFN-γ) mice, in which YFP reports transcriptional activity from the gene encoding IFN-γ. YFP staining was spontaneously evident in over one-third of epidermal CD8 T cells 96 hours post challenge, whereas no staining was detectable among DETCs, Langerhans cell (LCs), or low numbers of tissue-intrinsic αβ T cells that could be distinguished from T_{RM} cells by their high expression of CD3, that is, $TCR\beta^+$ $CD3^{high}$ cells (see above) (Fig 1, *D*). Additionally, Yeti cells stimulated *ex vivo* were stained for intracellular IFN-γ to validate YFP as a surrogate marker for cytokine production (Fig E2, *F*). In sum, DNFB sensitization elicited systemic CD8 cells comprising T effector cells and T_{RM}-cell precursors that on epicutaneous challenge showed rapid, incremental maturation into epidermal T cells collectively displaying a T_{RM}-cell–associated phenotype with potential for IFN-γ production, and a gradation of CD5 expression consistent with a spectrum of polyclonal TCR signal strengths.[22,23]

Dysregulated T_{RM}-cell elicitation in hapten-challenged γδ T-cell mutant mice

Because it was reported that $TCR\delta^{-/-}$ mice show exaggerated ACD responses,[9] we examined 3 strains of γδ T-cell mutant mice for the phenotypes of ACD-elicited epidermal CD8 T cells following sensitization and challenge. The strains were Tac, which specifically lack canonical $V\gamma5V\delta1^+$ DETCs because of a mutation in *Skint1*, the obligate DETC-selecting determinant;[5,45] $TCR\delta^{-/-}$ lacking all γδ T cells; and $V\gamma5V\delta1^{-/-}$ lacking canonical $V\gamma5V\delta1^+$ DETCs. In all strains of DETC-deficient mice, the percentage representation and absolute numbers of epidermal $CD8^+CD5^+$ T_{RM} cells were significantly greater, particularly following a second DNFB challenge 3 weeks after the first (Fig 2, *A* and *B*). Furthermore, $CD8^+$ T cells recovered from mice specifically lacking Vγ5Vδ1 DETCs showed significantly increased levels of expression of T-effector-cell–associated markers, including TNFRSF9 (or 4-1BB), NKG2D, and the integrin CD49a (ITGA1) (see Fig E3, *A* in this article's Online Repository at www.jacionline.org).

Both Tac and $V\gamma5V\delta1^{-/-}$ strains harbor "replacement" DETCs expressing a range of noncanonical γδ TCRs, whereas replacement DETCs in $TCR\delta^{-/-}$ mice comprise $TCR\alpha\beta^+$ CD8 cells that are distinguishable from CD8 T_{RM} cells because they are $CD8^{lo}$ and do not express CD5 (Fig 2, *A*; compare upper with lower right-most panels). Because of these replacement DETCs, greater T_{RM}-cell expansion in γδ-deficient settings could not easily be ascribed to there being an empty niche to fill (see below). Nonetheless, to avoid the issue of replacement T cells, we adoptively transferred CD8 T cells from Yeti mice to either $TCR\beta^{-/-}$ mice or $TCR\beta\delta^{-/-}$ mice that were then sensitized and subsequently challenged (Fig 2, *C*). By comparison to epidermal CD8 cells recovered from $TCR\beta^{-/-}$ recipients, those recovered from $TCR\beta\delta^{-/-}$ mice expressed significantly higher levels of T-effector cell markers including NKG2D, ICOS, 4-1BB, and NKG2A (Fig 2, *D*), comparable to the findings with $V\gamma5V\delta1^{-/-}$ mice. Additionally, the cells' YFP-fluorescence was higher indicating increased *Ifng* transcription (Fig 2, *E*), and they expressed significantly lower CD5 levels (Fig 2, *F*), as was the case for

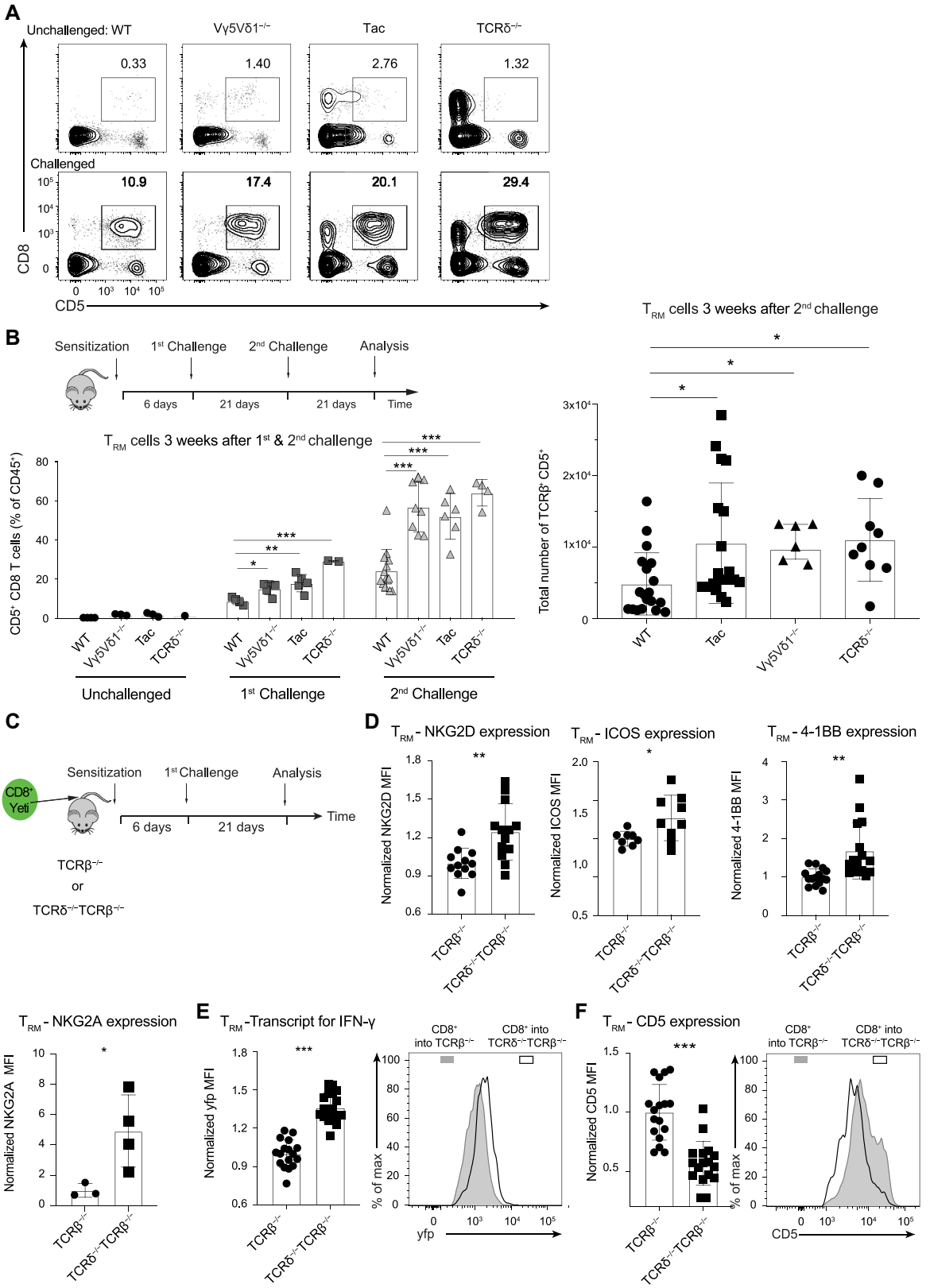

FIG 2. Dysregulated T_{RM}-cell elicitation in hapten-challenged γδ T-cell mutant mice. **A,** Representative CD8 and CD5 expression in CD45$^+$ cells from WT, Vγ5Vδ1$^{-/-}$, Tac, and TCRδ$^{-/-}$ mice either unchallenged (*upper*) or 21 days post sensitization and first challenge (*lower*). **B,** (*Left*) Protocol for sensitization and challenge (*upper*) and T_{RM}-cell frequencies after indicated challenges (*lower*). (*Right*) TCRβ$^+$CD5$^+$ counts 21 days after second challenge of strains shown; data from 3 independent experiments, n = 40 mice; data are mean ± SD;

epidermal T-effector cells maturing in mice exposed only once to DNFB without prior sensitization (see Fig 1).

Thus, across a range of mouse strains and experimental setups, a consistent pattern emerged by which CD8 T cells elicited by ACD in the absence of canonical, tissue-intrinsic γδ T cells showed greater numbers, higher effector potentials, and lower CD5 expression. The relationship between the frequency of elicited $CD8^+$ T_{RM} cells and inflammatory pathology was evident from their comparable dose-dependent responses to amounts of hapten applied (Fig E3, *B*), with ear thickness in $TCR\delta^{-/-}$ mice being significantly exaggerated even at a low dose (0.125%) of hapten (Fig E3, *C*).

Finally, the dysregulated elicitation of local $CD8^+$ T cells in $TCR\delta^{-/-}$ mice was strikingly phenocopied independently of ACD by inoculating mice with the squamous cell carcinoma line, PDV.[46] Thus, when $TCR\delta^{-/-}$ versus WT mice were inoculated, the influx of epidermal $CD5^+CD8^+$ T cells was significantly larger (Fig E3, *D*), but a significantly smaller proportion of the cells was $CD5^{hi}$ (Fig E3, *E*).

Tissue-intrinsic γδ T cells regulate the status of ACD-elicited CD8 T cells

To better understand the regulation of epidermal CD8 T_{RM}-cell formation by local γδ T cells, we compared the phenotypes of CD8 T cells at 72 hours after a second DNFB challenge of WT mice versus age-matched Tac mice (see above). Guided by the signature surface-marker phenotype described for ACD-elicited epidermal CD8 T cells, freshly isolated CD8 T cells from challenged WT and Tac mice were flow-sorted for $CD45^+TCR\beta^+CD103^+CD5^+$ cells (Fig 3, *A*) and subjected to 3′ mRNA single-cell transcriptomics, obtaining 483 mean reads per cell for the WT sample and 1346 for the Tac sample, with the top-most 1000 variably expressed genes selected for each. Sequencing saturation was >90% for all samples, indicating comprehensive sampling of available transcripts. After preprocessing, normalization, and batch correction, integrated analyses were applied to discriminate common cell types and facilitate comparative analyses, as described.[47] The application of t-SNE to a mixed data set from challenged WT and Tac mice permitted 5 distinct lymphocyte clusters to be discriminated according to their aggregate gene expression profiles (Fig 3, *A*).

For the purposes of illustration, the 10 genes whose expression was most enriched in the respective clusters are denoted (Fig 3, *B*), whereas the complete information is provided online (GEO accession number: GSE164023). The most prominent clusters were 2 $Cd8\alpha^+$ T cell clusters, cluster 1 and cluster 2, which will be further considered below; cluster 3 comprised a small group of $Cd4^+$ T cells enriched in regulatory T (T_{reg}) cell–associated transcripts; cluster 4 comprised contaminating $Cd3^-TCR\beta^-$ innate lymphoid cells; and cluster 5 comprised a very minor group of *Cd3*-expressing cells of uncertain classification, but note that they were not $TCR\gamma\delta^+$.

Accepting a false discovery rate of <1%, the largest grouping was cluster 1 (GSE164023) (Fig 3, *A* and *B*) displaying a prototypic T_{RM}-cell signature that is conserved in mice and humans and that includes *Cxcr6*, *Cd8a, Itgae* (encoding CD103), *Pdcd1* (encoding PD1), *Ccl4,* and *Cd69* (Fig 3, *B* and see Fig E4, *A* in this article's Online Repository at www.jacionline.org).[2,48] Additionally, genes associated with activated CD8 T-cell effector responses were highly expressed, including *Gzmb, Icos, Tnf,* and *Ifng* (Fig E4, *A*). Conversely, cluster 1 showed scant expression levels of genes associated with lymph node-homing and T effector memory cells, including *Sell* (encoding CD62L), *Ccr7, S1pr1*, *S1pr5*, *Klrg1,* and *Klf2* (GSE164023) (Fig E4, *B*).[2,48,49]

In many respects cluster 2 cells shared the collective cluster 1 T_{RM}-cell signature (GSE164023) (Fig E4, *A*), but they were uniquely enriched in RNAs associated with active cell cycling, including *Stmn1* (encoding stathmin1), *Tubb5*, *Rrm2* (encoding ribonucleoside-diphosphate reductase subunit M2), and *Mki67* (encoding Ki67, which is a marker of cells outside of G_0) (Fig 3, *B* and Fig E4, *C*).[50] Moreover, cluster 2 was strongly enriched in RNAs associated with the S and G_2-M phases of the cell cycle by contrast to a scarcity of RNAs associated with G_0 and G_1 (Fig 3, *C*). Thus, the epidermis at 72 hours after the second challenge concurrently housed resting (cluster 1) and cycling (cluster 2) $CD8^+$ T_{RM} cells.

We next compared how the epidermal T cells recovered from Tac versus WT mice at 72 hours post challenge were distributed across these clusters (Fig E4, *D* and *E*). There was a relative loss in Tac of cells from minor clusters 3 and 4 that evidently reflects fewer contaminating T_{reg} and innate lymphoid cells, but besides this, the major ACD-elicited epidermal CD8 T-cell subtypes (clusters 1 and 2) were comparably elicited in the absence of prototypic DETCs and in equivalent ratios. Nonetheless, Tac-derived CD8 T cells showed significant quantitative shifts in the expression of specific gene-sets. For example, at single-cell resolution, Tac-derived cluster 1 cells showed increased normalized counts (reflecting levels of expression) for genes associated with cytolytic effector functions, including *Ctla2a, Nkg7, Ctsw, Klrk1*, and signaling status including *Ptpn6* (encodes Shp1) and *Ptprcap*, both of which encode regulators associated with the modulation of highly activated T cells (Fig 3, *D*).[51,52]

Likewise, cluster 2 CD8 T cells from Tac mice showed striking increases in normalized counts retrieved for genes associated with cytotoxicity, including *Ctsw* and *Nkg7*; with mitosis, including *Stmn1, Tuba1b, Tubb5, Rrm2,* and *Hmgb1*; with outcomes of TCR signaling; and with oxidative phosphorylation; and as well as *Ccl8,* which also reflects activation (Fig 3, *E* and *F*). The increase in mitosis-associated genes is clearly consistent with the increased numbers of elicited $CD8^+$ T cells in γδ mutant mice. Conversely, cluster 2 CD8 T cells from Tac mice showed relatively reduced expression of genes associated with responsiveness to cytokines (Fig E4, *F*), an issue returned to below. In sum, the status of polyclonal epidermal CD8 T cells elicited by ACD in mice lacking canonical γδ DETCs was atypical, with greater

1-way ANOVA with Holm-Sidak's *post hoc* test. **C,** ACD protocol following adoptive transfer of YFP-Yeti $CD8^+$ T cells to $TCR\beta^{-/-}$ and $TCR\delta^{-/-}TCR\beta^{-/-}$ recipients. **D,** Normalized surface expression by transferred $CD8^+$ cells of indicated proteins. **E,** (*Left*) Normalized T_{RM}-cell expression of YFP; (*right*) representative YFP expression by intravenously transferred $CD8^+$ cells. **F,** (*Left*) Normalized T_{RM}-cell expression of CD5; (*right*) representative CD5 expression by intravenously transferred $CD8^+$ cells. **D-F,** Data from 3 independent experiments, n = 33 mice. Data are mean ± SD; Student *t*-test. $*P < .05$, $**P < .01$,$***P < .001$.

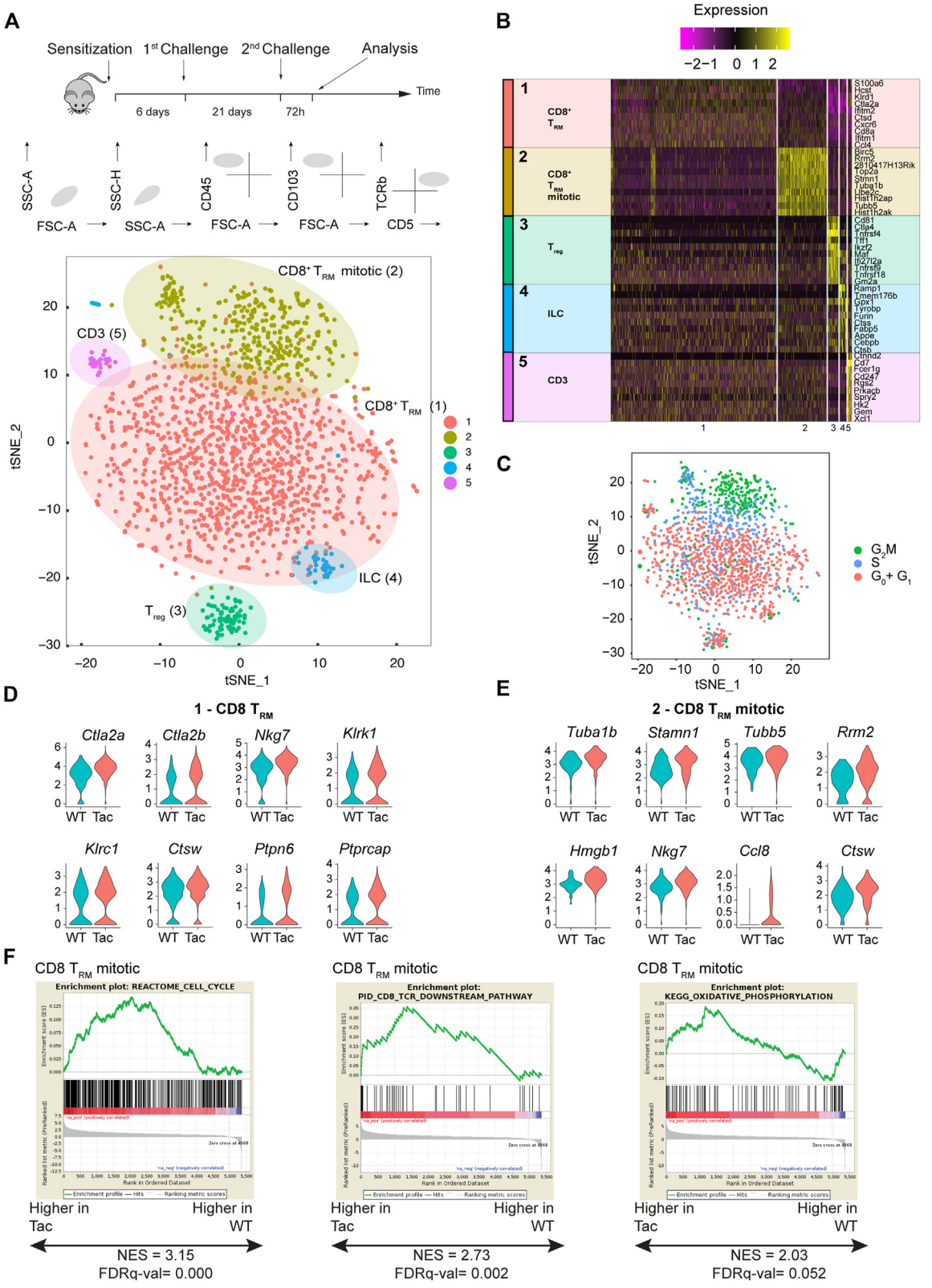

FIG 3. Tissue-intrinsic γδ T cells regulate the status of ACD-elicited CD8 T cells. **A-F,** scRNA-seq analysis of $CD8^+$ T cells from WT and Tac mice 72 hours after first challenge. **A,** ACD experimental protocol and workflow for isolating cells (*upper*); t-SNE plot demarcating 5 clusters based on differentially expressed genes for 1829 cells passing quality control (WT + Tac); numbers in parentheses correspond to clusters listed in panel **B. B,** Heat map for cells grouped into 5 indicated clusters; the 10 genes most highly differentially expressed by each cluster are denoted (*right*). **C,** t-SNE plot of scRNA-seq data set reflecting cell cycle analysis. **D,**

cytolytic effector potentials that phenocopied CD5^{dim}NKG2D^{hi} effector T cells observed in mice exposed to DNFB without prior sensitization (see Fig 1), and higher proliferative activity previously reported for CD5^{lo} T_{RM} cells that generally have lower TCR affinities relative to CD5^{hi} T_{RM} cells.[42,53]

ACD concurrently elicits local γδ T-cell activation

To understand how local γδ T cells might regulate T_{RM}-cell maturation, it was important to ask whether ACD concurrently induced DETC activation, creating a context in which epidermal CD8 T-cell differentiation would occur. At steady-state, Vγ5Vδ1$^+$ DETC-specific epithelial selecting elements, Skint1 and Skint2, maintain canonical DETCs in an activated-yet-resting state.[17] However, RNAs encoding *Skint2*, and to some extent *Skint1*, were rapidly downregulated in DNFB-treated mice (Fig 4, *A*), and by 72 hours post challenge of sensitized mice, at a time of heightened T_{RM}-cell maturation (exemplified by CD5 and CD103 upregulation), most DETCs displayed a fully activated phenotype reflected by increased sphericity and CD69 upregulation (Fig 4, *B*, arrows; and see Fig E5, *A* and *B* in this article's Online Repository at www.jacionline.org). By contrast, replacement, noncanonical DETCs in Tac mice showed much reduced activation in response to DNFB (Fig E5, *B*). Indeed, the activated phenotype in WT mice was that of *bona fide* DETCs, because those cells uniquely express Vγ5 and there was no evidence of epidermal infiltration by γδ T cells using other TCRs, for example, Vγ4, which is common among dermal γδ T cells,[54] or Vγ1, which is common among so-called replacement DETCs that can commonly be found in the epidermis of Vγ5Vδ1-deficient mice (Fig E5, *C*).

At a higher level of resolution, there were profound differences in the gene expression profiles of Vγ5Vδ1$^+$ DETCs recovered 72 hours after challenging sensitized mice versus those at steady-state, as illustrated by a principal component analysis (PCA) of an RNA-seq analysis (GSE164023) (Fig 4, *C*; see Table E1 in this article's Online Repository at www.jacionline.org). Specifically, by 72 hours many mRNAs associated with T-cell activation were increased, including those encoding cytokines, cytokine receptors, selected chemokines, key cytolytic mediators, and costimulatory and coinhibitory receptors, for example, 4-1BB, ICOS, and Tim3 (Fig E5, *D*). Conversely, some mRNAs strongly expressed at steady-state, for example, *Id3* and *Xcl1*, were decreased (Fig E5, *D*).

IFN-γ contributes to local γδ T-cell activation

Within the highly activated profile of DETCs recovered 72 hours after challenge, we noted conspicuous upregulation of many IFN-γ–responsive genes, including *Ly6a, Stat1, Cxcl10* (encodes IP10), and *Cd274* (encodes PD-L1) (Fig E5, *E*). Strikingly, by comparison to keratinocytes and LCs, DETCs were the intraepidermal cells most consistently expressing RNA and protein for the 2 chains of IFNGR that are both required for IFN-γ responsiveness (GSE160477) (Fig 4, *D*; Fig E5, *F*).[55] Consistent with this, a significantly greater fraction of DETCs versus LCs were responsive to IFN-γ, as measured by *Sca1* upregulation (Fig E5, *G*).[56] Therefore, we next investigated the DETC response to ACD in mice lacking IFNGR (CD119). DETCs entirely failed to show PD-L1 upregulation when sampled every 24 hours for 4 days following challenge of sensitized *Ifngr1*$^{-/-}$ mice (Fig 4, *E*), and a PCA of DETCs from *Ifngr1*$^{-/-}$ versus WT mice sampled at 72 hours following DNFB challenge showed them to express substantially different transcriptomes (GSE164023) (Fig 4, *F*; see Table E2 in this article's Online Repository at www.jacionline.org), including reduced expression of *Stat1, Tbx21* (encodes T-bet), and *Ly6a*, and ablated PD-L1 (Table E2). We could therefore conclude that during ACD, the local γδ T-cell phenotype is in part regulated by IFN-γ. Strikingly, sensitized and challenged *Ifngr1*$^{-/-}$ mice phenocopied γδ mutant mice in displaying increased frequencies of elicited CD8 T cells (Fig 4, *G*), a result that is at least consistent with the hypothesis that the impact of IFN-γ on ACD was mediated via local γδ T cells.

To test this hypothesis, we generated an inducible γδ-specific *Ifngr2*-deficient mouse strain by crossing a floxed allele of *Ifngr2* with a mouse expressing a tamoxifen-responsive cre-recombinase (CreER) under the control of the TCRδ promoter (Fig 4, *H*). In the epidermis, this would preclude the upregulation of IFN-γ–dependent genes specifically in DETCs. The penetrance of TCRδ^{CreER}-mediated deletion is almost 100% in skin γδ T cells, by contrast to γδ T cells at other sites,[29] and this was reflected in their loss of Ifngr protein expression (Fig E5, *H*), and their greatly reduced capacity to upregulate *Sca1* in response to IFN-γ (Fig E5, *I*). Strikingly, the ACD response of these mice phenocopied the ACD response of DETC-deficient mice and *Ifngr*$^{-/-}$ mice, in that there was a highly exaggerated elicitation of CD8 T cells that expressed significantly lower levels of CD5 and significantly higher levels of effector T-cell–associated proteins including NKG2D (Fig 4, *I*). Thus, the phenotype of local, ACD-elicited CD8$^+$ αβ T_{RM} cells was significantly affected by the targeted deletion of a single gene (*Ifngr*) in an heterologous cell type (DETC). Moreover, because the DETC compartment is full in TCRδ^{creER}*Ifngr*$^{fl/fl}$ mice, this observation emphasizes the point that increased T_{RM}-cell frequencies cannot be explained simply by a loss of local γδ T cells creating an empty niche.

Based on the data using Yeti mice, we next considered that ACD-elicited epidermal CD8$^+$ T cells might be a local and sustained source of IFN-γ to which DETCs respond during ACD. Indeed, IFN-γ is reportedly most active within close proximity of its cellular source.[57] Seemingly consistent with this, when whole epidermis was harvested from ACD-challenged mice and rested for 48 hours, >80% of TCRγδ$^+$ cells expressed PD-L1, whereas explanted γδ T cells that were first flow-sorted prior to

Violin plots comparing expression of genes associated with cytotoxicity and signaling in cluster 1 cells from WT (*green-blue*) and Tac (*pink*) mice. **E,** Violin plots comparing expression of genes associated with cytotoxicity and proliferation in cluster 2 cells from WT (*green-blue*) and Tac (*pink*) mice. **D,E,** Shown are violin-shaped fitting areas for statistically significant differences in gene expression for T_{RM} cells from WT versus Tac mice. ***$P < .001$. **F,** Gene set enrichment analysis of T_{RM}-cell mitotic cluster from Tac versus WT backgrounds using indicated public gene sets: enrichment scores (*NES*) and *P* value are reported. *FDR,* False discovery rate; *FSC-A,* forward scatter area; *SSC-A,* side scatter area; *SSC-H,* side scatter height.

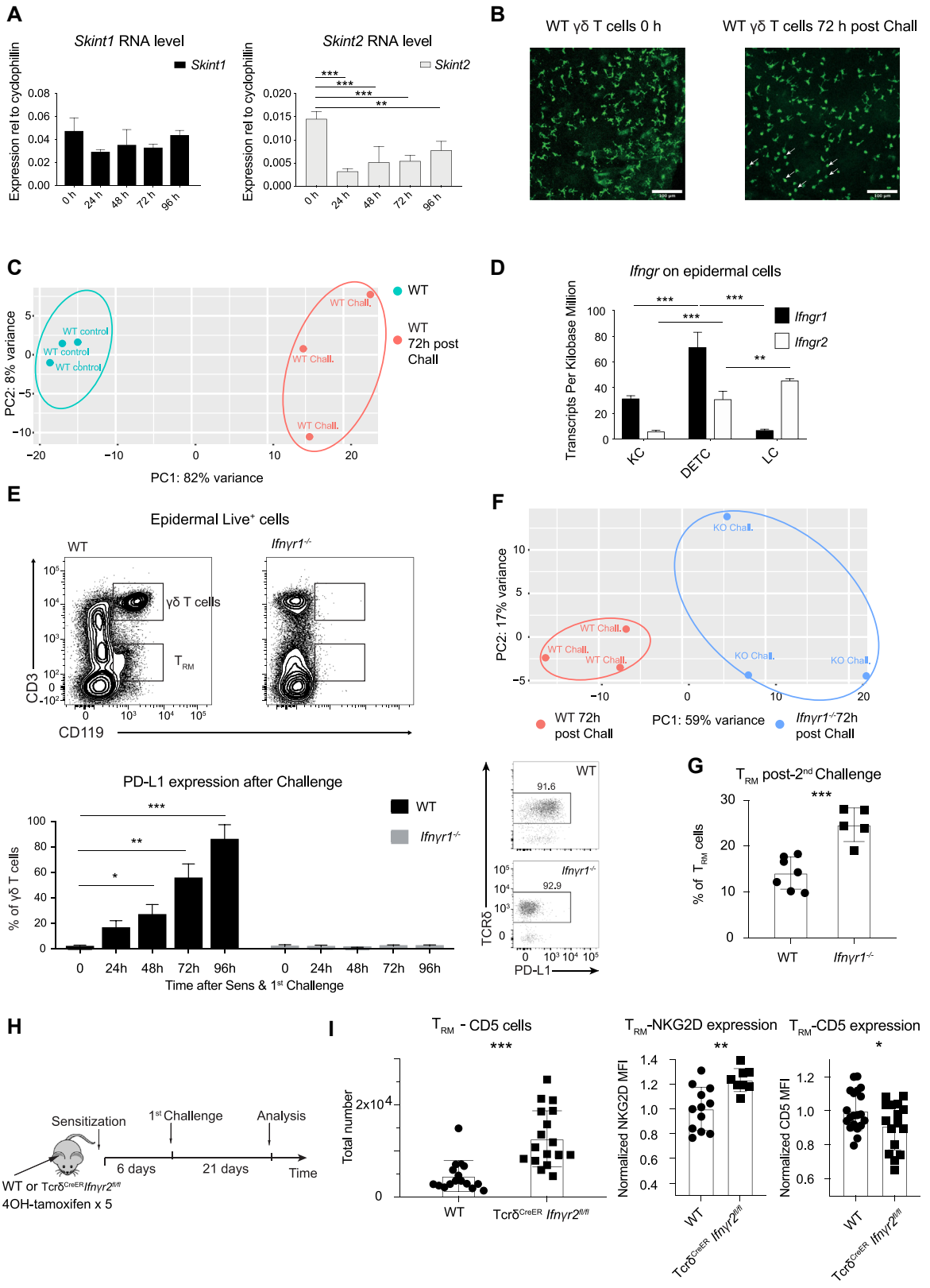

FIG 4. ACD concurrently elicits local γδ T-cell activation. **A,** *Skint1* and *Skint2* expression after sensitization and first challenge; n = 3; data are mean ± SD of a representative of 2 independent experiments. **B,** DETCs stained for TCR-γδ (*green*) in unchallenged WT mice or 72 hours post first challenge; representative of 3 independent experiments. *Arrows* denote rounded cells. **C,** PCA of RNA-seq analysis of γδ cells from unchallenged mice (n = 3) or 72 hours after first challenge (*Chall*) (n′ = 3). **D,** *Ifngr1* and *Ifngr2* transcript counts by indicated cell types from unchallenged mice (n = 3). **E,** (*Upper*) CD3 and CD119 (IFNGR1) expression on

being maintained in culture mostly became PD-L1^{neg} (Fig E5, *J*). Further evidence that DETCs respond to IFN-γ produced by local αβ T cells was provided by exposure of the 48-hour explant cultures to low concentrations of an activating anti-TCRβ antibody, H-57, which induced DETCs to display increased phosphorylation of STAT1 that is downstream of IFNGR engagement. Moreover, this was increased further when the cultures were explanted from challenged mice (Fig E5, *K*).

These observations would be consistent with locally maturing CD8 T cells and activated tissue-intrinsic γδ T cells being connected by an IFN-γ–dependent feedback loop, akin to a "sensing and alarm" function by which T_{RM} cells condition the immunological tenor of local tissues.[58] Whereas αβ T_{RM} cells would activate DETCs via IFNGR, activated DETCs might reciprocally regulate αβ T_{RM} cells via PD1, which was highly expressed by most elicited T_{RM} cells (see Fig 1). At least consistent with this, anti-PD-L1–treated mice showed increased ear swelling 72 hours post challenge, relative to controls (Fig E5, *L*), as was also recently reported for *Pdl1*$^{-/-}$ mice.[59] Thus, we next sought evidence that ACD-elicited CD8 T cells directly interacted with DETCs. Note that this would not conflict with the report that epidermal areas occupied by T_{RM} cells and DETCs were largely nonoverlapping at steady-state because those observations were made some weeks following *Herpes* virus-induced T_{RM}-cell formation.[7]

Local γδ T cells interact with ACD-elicited CD8 T cells *in vivo*

To interrogate whether direct DETC–CD8 T-cell interactions were occurring, we applied confocal microscopy to vital epidermal sheet preparations from the ears of Yeti mice at 72 hours post challenge, detecting YFP as a surrogate of IFN-γ–producing cells (see above, and staining with antibodies against CD8 and TCRγδ, respectively (Fig 5, *A*). High densities of CD8 T cells were visualized at the challenge site, many of which expressed YFP (that could be sufficiently bright as to diminish the CD8 signal) (Fig 5, *A*, red), and many of which were intimately juxtaposed with DETCs, including those expressing PD-L1 (Fig 5, *A*, blue; arrowed; Fig 5, *B*, white; Fig 5, *C*; see Video E1 in this article's Online Repository at www.jacionline.org).

A potent, relatively underexplored consequence of PD-L1/PD1 engagement is the markedly increased motility of PD1$^+$ T cells. Thus, in the context of type I diabetes, enhanced PD-L1–dependent motility of pancreatic islet antigen-specific TCRαβ$^+$ cells within tissue-draining lymph nodes was interpreted as promoting tolerance by restricting antigen/TCRαβ-dependent "strong-stop" contacts with dendritic cells to only those T cells with the highest affinity TCRs, that is, the highest quality T cells.[60] By contrast the activation of lower affinity T cells, which is a common trait of autoreactive T cells, would be physically limited by enhanced PD-L1–dependent motility. Indeed, greatly enhanced PD1-dependent T-cell motility was observed during tissue regeneration following oncogene-induced tissue injury and was interpreted as promoting tolerance by limiting αβ T-cell interactions with damaged and proliferating cells.[61] We therefore investigated the regulated motility of epidermal CD8$^+$ T cells following induction of ACD and the potential roles that DETCs and PD-L1 might play.

To this end, we employed CXCR6^{GFP} mice in which DETCs at steady-state are GFP$^+$, as are tissue-infiltrating CD5$^+$CD8$^+$ αβ T cells following challenge (see Fig E6, *A* in this article's Online Repository at www.jacionline.org). Those mice were crossed to homozygosity for TCRβ–deficiency, so that now DETCs were the only epidermal GFP$^+$ cell type, and those mice were then reconstituted with CD8$^+$ αβ T cells that could be distinguished from DETCs because they were from TdTomato mice. Those recipients were sensitized and at 72 hours post challenge their ears were assessed by intravital confocal microscopy (Fig 5, *D*). Green cells (ie, DETCs) were essentially sessile, as previously reported,[6] with the motility of tracked cells being captured at every 30 seconds over a time frame of 60 minutes (ie, 120 steps) by a circle with an average radius of 1.02 ± 0.18 mm (Fig 5, *E*). By contrast, red (CD8) cells were captured in the same time frame by a circle of radius 14.17 ± 2.97 mm, attesting to their motility (Fig 5, *F*). Moreover, there were clear instances of motile CD8 T cells making episodic and repeated interactions with DETCs (see Video E2 in this article's Online Repository at www.jacionline.org). Analyzed in greater detail, the CD8 cells showed an average step size (the distance measured in each 30-second interval) of ~3.5 mm and no skewed directionality. Nonetheless, their mean square displacement from their start positions did not increase linearly with time (ie, their velocity was not uniform), with some restraint on motility, particularly in early imaging intervals, as evidenced by negative deviation from the straight line (Fig 5, *F*; see Video E3 in this article's Online Repository at www.jacionline.org).

To better understand this motility pattern, we composed several simulations in which a red motile cell was positioned among sessile green cells precisely modeling the arrangement of cells observed in the tissue by microscopy. We assigned several value functions, reflecting: (1) the random movement of the cells in terms of displacement (0.0-1.0) and direction (0°-360°); (2) their hypothetical activation by an initiation factor, for example, a response to PD-L1 engagement that would increase step size (0.99); and (3) their hypothetical attraction to a nearest neighboring DETC within 100 mm (0.7) that would affect cell direction. Additionally, we imposed a maximum step size of 14 mm based on our real-world observations, and we included terms to simulate potential contacts between the 2 cell populations, operative where 2 cells are <3 mm apart. To a striking degree, this simulation phenocopied the data obtained from tracking epidermal CD8 T cells following DNFB challenge (compare Fig E6, *B* with Fig 5, *F*). Moreover, by observing 40 CD8 T cells

epidermal cells from WT and *Ifnγr1*$^{-/-}$ mice (3 independent experiments); (*lower*) frequency of PD-L1–expressing epidermal γδ cells at indicated times post sensitization and first challenge, with representative plot of CD45$^+$ epidermal cells at 96 hours. **F,** PCA of RNA-seq analysis of epidermal γδ cells sorted 72 hours after sensitization and first challenge of WT (n = 3) or *Ifngr1*$^{-/-}$ mice (n′ = 3). **G,** T_{RM}-cell frequency in WT (n = 7) and *Ifngr1*$^{-/-}$ mice (n = 5) 21 days post second challenge; data are mean ± SD of 2 independent experiments; Student *t*-test. **H,** Protocol for γδ-specific *Ifngr2* deletion, followed by ACD. **I,** T_{RM}-cell counts and normalized T_{RM}-cell surface expression of denoted proteins; data from 3 biologically independent experiments, n = 36 mice; Student *t*-test. **A,D,E,** Statistical analysis performed using 1-way ANOVA with Holm-Sidak's post-hoc test. **D,** Only statistical comparisons with DETCs are shown. **P* < .05, ***P* < .01,****P* < .001.

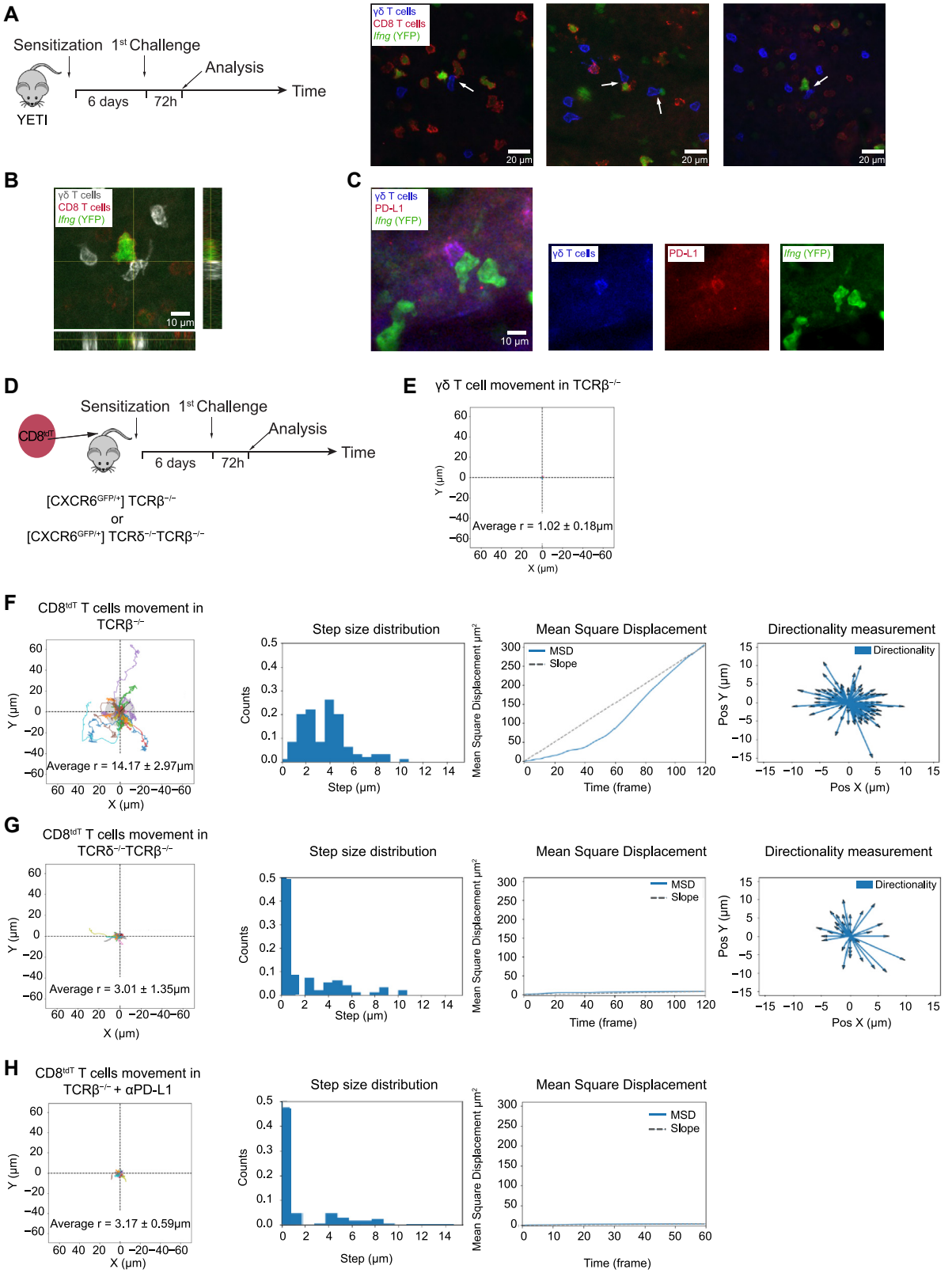

FIG 5. Local γδ T-cell interactions with ACD-elicited CD8 T cells *in vivo*. **A,** ACD experimental protocol (*left*). **A-C,** Confocal microscopy images of ear epidermal sheets of YFP-Yeti mice (n = 3) stained as indicated; *arrows* denote juxtaposed cells. **D,** Protocol for adoptive transfer of tdTomato-CD8^{+} cells to CXCR6$^{GFP/+}$.TCRβ$^{-/-}$ or CXCR6$^{GFP/+}$.TCRβ$^{-/-}$TCRδ$^{-/-}$ mice followed by ACD. **E,** Confocal microscopy cell migration tracks of individual CXCR6$^{GFP/+}$ γδ cells normalized for their origin. **F-H,** Confocal microscopy cell migration tracks of individual tdTomato T_{RM} cells in the skin normalized for their origin. The *gray circle* radius is the weighted

in a given field-of-view containing sessile DETCs, the model permitted us to estimate that ~25% of CD8 T cells would be in contact with DETCs over the 60-minute time frame (Fig E6, *C*).

Given that the simulation so closely phenocopied the cell tracking data, we tested some key components of it. First, CD8 T-cell movement in the absence of γδ T cells might be significantly altered by both a lack of a γδ T-cell–dependent PD-L1–dependent activation function, and a lack of an attraction function. Thus, we repeated the study by using TdTomato CD8 αβ T cells to reconstitute $CXCR6^{GFP}$ $TCR\beta\delta^{-/-}$ mice that lacked all T cells and that were then sensitized and challenged. Indeed, at 72 hours post challenge, CD8 T-cell motility ($r = 3.01 \pm 1.35$ mm) was much reduced relative to that observed in γδ-sufficient mice (compare Fig 5, *G* with Fig 5, *F*). Furthermore, the modal step size was 0, reflecting the fact that there was negligible mean square displacement (Fig 5, *G*), and the rare instances of motility showed no directional skewing. These observations were strikingly phenocopied by a simulation in which the activation and attraction functions were assumed to be negligible (compare Fig E6, *D* with Fig 5, *G*).

We next investigated whether motility post-ACD was PD-L1–dependent by administering anti-PD-L1 antibody 24 hours prior to DNFB challenge of presensitized $CXCR6^{GFP}$ $TCR\beta^{-/-}$ mice reconstituted with TdTomato CD8 T cells. Indeed, the cells' movement was greatly impaired by anti-PD-L1 ($r = 3.17 \pm 0.59$ mm; modal step size = 0) (Fig 5, *H*), closely phenocopying the setting of γδ T-cell deficiency, just as the significantly increased ear swelling responses to DNFB challenge of anti-PD-L1–treated mice phenocopied those of γδ T-cell deficient mice. We can conclude that following ACD, the high motility of elicited T_{RM} cells was equally dependent on local γδ T cells and on PD-L1 that was primarily expressed by local γδ T cells, dependent on their activation by IFN-γ, for which the primary source was local $CD8^+$ αβ T cells. We note, however, that despite their failure to upregulate CD69 (see Fig E5, *B*), replacement DETCs in post-challenge Tac upregulated PD-L1 (Fig E6, *E*), which clearly indicates that although PD-L1 is essential for regulating CD8 T-cell motility (Fig 5, *H*), it cannot be sufficient.

Mouse and human γδ T and T_{RM} cells *in vitro*

Next, we examined the capacity of DETCs to regulate T_{RM}-cell formation *in vitro*. These studies were rooted in our observation that a T_{RM}-cell signature could be induced in circulating T cells from mice 5 days post-DNFB sensitization following 2 days' exposure *ex vivo* to 2 epithelium-associated cytokines, TGFB and IL15, whereas this induction was much less efficient for splenic CD8 T cells from unchallenged WT mice (~45% conversion compared to ~15%). This was evidenced by the cytokine-dependent acquisition of CD103, and by CD5 upregulation, which was mostly a trait of $CD103^+$ cells (see Fig E7, *A-C* in this article's Online Repository at www.jacionline.org). This phenotypic change was further enhanced by TCR stimulation (Fig E7, *D*), and it is noteworthy that CD103 upregulation was limited to $KLRG1^-$ CD8 T cells (Fig E7, *E*), which are reportedly the near-exclusive source of T_{RM}-cell progenitors.[39,62]

Based on this, we repeated the cytokine-supplemented cultures of splenic CD8 T cells from sensitized and challenged mice, but in addition interrogated whether γδ T cells could directly influence T_{RM}-cell regulation. Thus, we added to the cocultures short-term lines of $V\gamma5V\delta1^+$ DETCs, established as previously described,[63] observing significant increases in the fraction of CD8 T cells expressing CD103, and those cells expressed significantly higher CD5 levels (Fig 6. *A*). Interestingly, $CD5^{lo}$ versus $CD5^{hi}$ CD8 T cells were reported to respond less well to cytokines and to show increases in outcomes associated with TCR signaling,[53] which were precisely those traits deduced from the transcriptomic analysis of T_{RM} cells from γδ−deficient mice as described above. Thus, canonical DETCs can directly influence the acquisition of a T_{RM}-cell signature in the absence of any other cell types *in vitro*.

We then sorted ~2×10^4 T_{RM}-type CD8 T cells into culture with very low concentrations of activating anti-TCRβ antibody, H57, sufficient to sustain the cells with moderate, albeit variable levels of expansion over a 3-day period (Fig 6, *B*; left panels). Coculture with short-term DETC lines significantly limited CD8 T-cell expansion (Fig 6, *B*; left), although it is clear from the live-dead analysis that the CD8 T cells remained >99% viable (Fig 6, *B*; middle panels). Strikingly, the DETC-imposed constraint on CD8 T-cell expansion was substantially and significantly relieved, by inclusion of anti-PD-L1 versus inclusion of an isotype control, whether measured as cell frequencies or as absolute numbers (Fig 6, *B;* top and bottom panels). Thus, substantially greater expansions of CD8 T cells were a common feature of T_{RM}-cell maturation in multiple settings of γδ deficiency, IFNGR deficiency, and PD-L1 blockade *in vivo* and in culture.

Next, we considered that if the findings described in this paper were to be conserved in human tissues, at least 2 key criteria should be fulfilled: first, that tissue-tropic or tissue-intrinsic γδ T cells should express PD-L1; and second, that this should be subject to regulation by IFN-γ, as is produced by human CD8 T cells. We focused initially on $V\delta2^+$ cells, because they are conspicuous in the dermis and epidermis within 48 hours of an ACD response to 2,4-dinitrochlorobenzene, in which context they have been postulated to regulate the ACD response post-initiation.[64] Skin-homing lymphocytes can be identified among PBMCs by their expression of cutaneous lymphocyte antigen (CLA),[65] and when we examined fresh $CLA^+V\delta2^+$ T cells from 4 independent healthy donors, we found that from ~15% to 40% were $PD\text{-}L1^+$, and that this invariably increased (from >35% to ~60% $PD\text{-}L1^+$) on exposure to IFN-γ (Fig 6, *C*). Hence, skin-homing γδ T cells implicated in ACD[64] are responsive to IFN-γ and upregulate PD-L1.

To examine the more general applicability of this to human barrier-site immunology, we examined human gut γδ intraepithelial lymphocytes, which are enriched in cells coexpressing Vδ1 and CD103.[66] Fresh populations of such cells from each of 3 donors (donors 1, 2, and 3) were cultured for 24 hours in standard media with and without IFN-γ. The data show that there was in each

mean of the track total displacements. Reported values for *r*: weighted mean ±SD of the weighted mean. **F,** $CXCR6^{GFP/+}TCR\beta^{-/-}$ mice: cells (n = 26) in 3 different experiments. **G,** $CXCR6^{GFP/+}TCR\beta^{-/-}TCR\delta^{-/-}$ mice: cells (n = 22) in 3 different experiments. **H,** $CXCR6^{GFP/+}TCR\beta^{-/-}$ mice + αPD-L1: cells (n = 20) in 3 different experiments. **F-H,** tdTomato-$CD8^+$ cells: step size distribution, mean square displacement (*MSD*), and directionality quantified using Manual Tracking plugin in Fiji[38] (*lower*). One representative experiment of 3 experiments performed is shown.

case a small percentage of cells that expressed PD-L1 and that in 2 of 3 donors, this fraction was increased by IFN-γ treatment (Fig 6, *D* and Fig E7, *F,* top panel).

To assess the generality of this yet further, we examined another site harboring intraepithelial γδ cells, namely the lung, for which nonlesional tissue was available from persons treated for non—small cell lung cancer. Although there were insufficient cells to culture, the data show that for each of 3 donors (donors 4, 5, and 6) a clear percentage of cells expressed PD-L1 and that this was in every case greater than the percentage expressed by $V\delta2^+$ cells (Fig E7, *F* [lower panel] and *G*). We conclude that in multiple barrier sites in which human $CD8^+$ T_{RM} cells mature, there exist local populations of γδ T cells displaying IFN-γ–regulatable expression of PD-L1.

DISCUSSION

T_{RM} cells exemplify the critical role played by local immune systems in responding to secondary challenges wrought by allergens, reinfections, and cancer recurrence. Their protective responses and pathological potentials can be long-lasting, added to which T_{RM} cells may also respond to primary challenges via TCR cross-reactivity and/or innate-like receptors.[67] It is therefore not surprising that T_{RM} cells would be locally regulated, consistent with which, skin T_{RM} cells are known to be influenced by keratinocytes,[68] and by local, T-bet–expressing $TCR\alpha\beta^+$ T_{reg} cells.[69] With this in mind, we revisited a potential for T_{RM}-cell regulation by local tissue-intrinsic lymphocytes that was described many years ago, but with no elucidated mechanism. Moreover, puzzlement over mechanism was increased by clear evidence that T_{RM} cells and DETCs were spatially isolated from one another when observed some weeks following epicutaneous *Herpes* infection.[7] However, this did not preclude an influence of DETCs in the early stages of ACD elicitation, when the CD8 T-cell population comprises effector cells and locally maturing T_{RM}-cell precursors. Indeed, as an example of early phase regulation, $CD8^+$ effector T cells accumulating at the intestinal barrier showed limited maturation toward a signature T_{RM}-cell phenotype when local T-bet–expressing $TCR\alpha\beta^+$ T_{reg} cells were lacking.[69]

Our study now establishes that during the early stages of epidermal infiltration in response to chemical challenge of presensitized mice, CD8 T_{RM}-cell maturation is comparably dysregulated by the absence of local γδ T cells, or of IFN-γ responsiveness (ie, in *Ifngr*$^{-/-}$ *mice)*, or of IFN-γ responsiveness induced purely in γδ T cells. We show that the CD8 T cells themselves are a primary source of IFN-γ, which is absolutely required to induce PD-L1 on local γδ T cells. Moreover, the phenotype of γδ T-cell–mediated regulation of CD8 T cells— regulated proliferation, effector function, and motility—is exactly that reported for checkpoint regulation by PD-L1, and the use of anti-PD-L1 blocked the direct regulation of CD8 T cells by γδ T cells that we could observe in culture. Consistent with this, local γδ T cells were in intimate contact with CD8 T cells soon after their elicitation.

Thus, the size and phenotype of the T_{RM}-cell compartment can be shaped by local innate-like lymphocytes in the early phases of ACD, and of other tissue-disruptive challenges as we show for the response to cancer cell inoculation. Moreover, the atypical phenotype of epidermal T_{RM} cells in the absence of DETCs included reduced CD5 expression that has been associated with lower intrinsic TCR affinity for antigen and higher propensity for autoreactivity and autoinflammation.[23] Thus, CD8 T cells entering a tissue en route to composing a T_{RM}-cell compartment encounter heterologous T cells that are themselves responding to the challenge (eg, ACD), evoking an immunological ecosystem. The likely conservation of this in humans is evident from the IFN-γ–dependent acquisition of PD-L1 by skin-homing γδ T cells, and by the expression of PD-L1 by tissue-intrinsic γδ T cells in the gut and lung.

Our findings may go some way to explaining many instances of inflammatory pathologies associated with γδ T-cell deficiencies.[11] Various etiologies have been considered to underpin such disease states, including dysbiosis caused by a deficiency in dermal IL17–producing γδ T cells.[70] Notwithstanding such causes, tissue-associated αβ T cells are a key effector of the described pathologies,[8,9] and this potential will clearly be exaggerated if local γδ T cells, by virtue of their absence, are unable to regulate the quality and size of the T_{RM}-cell compartment.

Innate-like lymphocytes including DETCs are commonly viewed as protecting tissue integrity, promoting repair, and limiting inflammation,[71,72] but there has been surprisingly little consideration of whether their biology might critically include the regulation and the establishment and maturation of T_{RM} cells. That these 2 qualitatively distinct tissue-associated lymphocyte universes are integrated rather than parallel has many implications. For example, given that the conditional ablation of a single gene in heterologous local γδ T cells (*Ifngr*) profoundly affected T_{RM}-cell maturation, it seems reasonable to consider tissue-intrinsic epidermal γδ T cells as *bona fide* immunoregulators. PD-L1 may be a major mediator of the critical role played by IFN-γ, conspicuously evoking the role of PD1 in suppressing T-effector cell function and promoting T_{RM}-cell maturation following virus infection of mouse lungs.[73] Nonetheless, we also show that PD-L1 is insufficient for T_{RM}-cell regulation, in which regard, DETCs express several molecules, including glucocorticoid-induced TNFR-related TNFRSF18 (GITR) protein, that have been associated with immunoregulation.[74] In short, the full regulatory potential of tissue-intrinsic T cells in different tissues merits much deeper investigation.

In considering the implications of local γδ T-cell–mediated T_{RM}-cell regulation by γδ T cells, we note that in mice adoptively transferred with T cells with lower intrinsic TCR affinity for influenza viruses, the durable lung T_{RM}-cell compartment that developed following influenza infection was smaller than that which formed in mice receiving higher affinity cells that also expressed higher levels of CD5.[42] Those data in the context of our own strengthen the prospect that tissue-intrinsic γδ T cells impose filters that bias the infiltrating CD8 T cells against expansion as short-term effector cells, commonly with lower TCR affinities, and toward maturation and expansion as higher affinity $CD5^{hi}$ T_{RM} cells. This bias toward high-quality T_{RM} cells imposed by tissue-intrinsic T cells may in part be via the regulation of T-cell motility that we demonstrate here, and that would limit activation of autoreactive T cells that escaped central tolerance based on their lower affinity.[75] In sum, local γδ T cells may deploy PD-L1/PD1 and other mediators to promote tissue-tolerance while nonetheless permitting sustained immune surveillance of exogenous threats by a selected population of high-quality cells. Consistent with this, αβ T-cell–dependent autoinflammatory diseases have been commonly observed in multiple strains of γδ-deficient and *Ifngr*-deficient mice.[8-10,12]

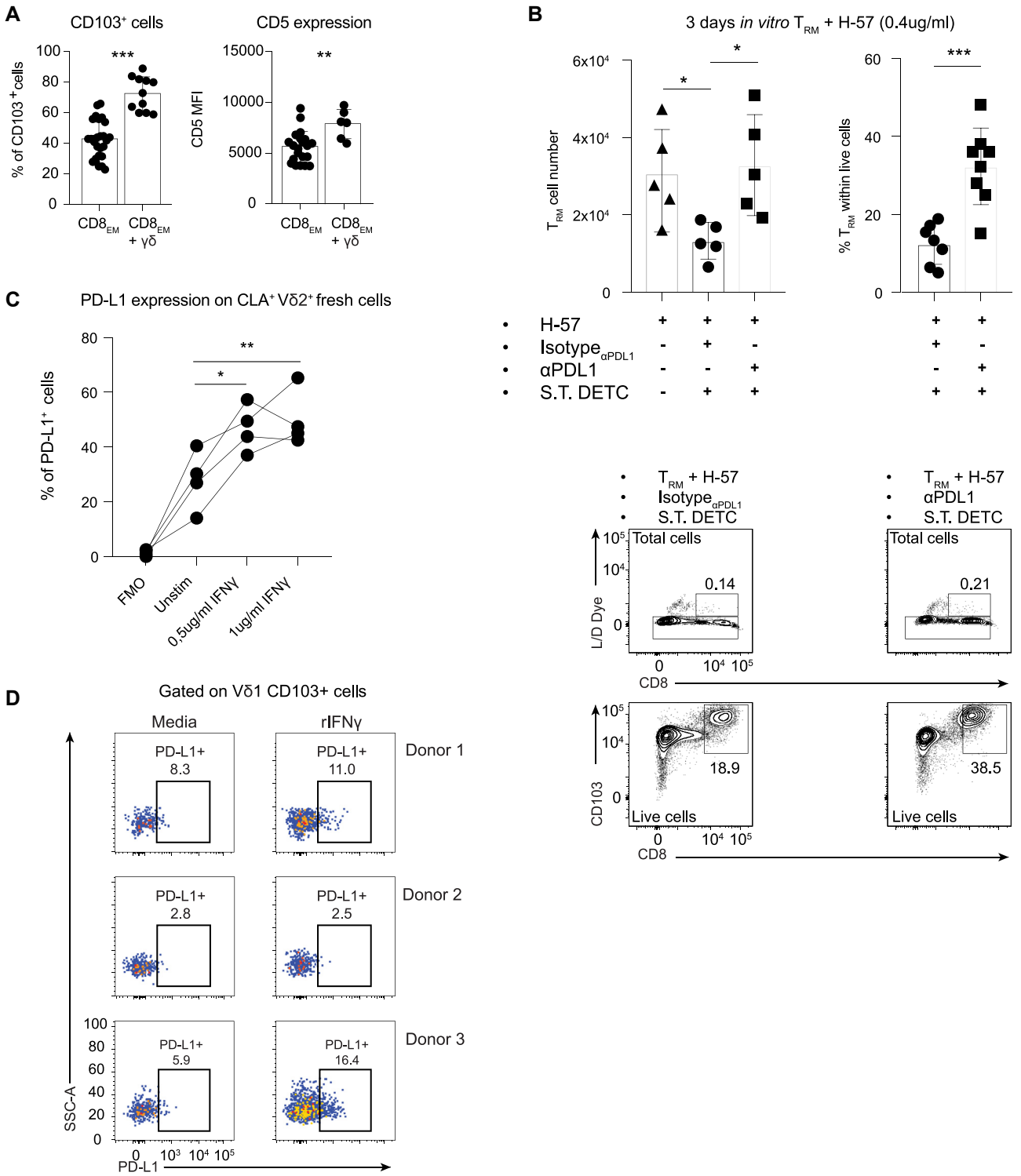

FIG 6. Mouse and human γδ T cells and T_{RM} cells *in vitro.* **A,** CD103 and CD5 expression by sensitized $CD8_{EM}$ cells after 3 days *in vitro* coculture with short-term (*S.T.*) DETCs (+ γδ) with TGFβ + IL15. Student *t*-test. **B,** (*Upper*) T_{RM}-cell frequencies and numbers after 3 days *in vitro* coculture of second challenge (T_{RM} + S.T. DETCs + H-57) performed in the presence of αPD-L1 blocking antibody (20 mg/mL) or isotype control (20 μg/mL) (*left*). Statistical analysis was performed using 1-way ANOVA with Holm-Sidak's multiple comparisons *post hoc* test. (*Lower*) Representative flow plots for live/dead plus CD8 and for CD103 plus CD8. **C,** Percentage of $PD\text{-}L1^+$ cells within blood $V\delta2^+CLA^+$ cells after 24 hours *in vitro* culture of human PBMCs with indicated concentrations of recombinant IFN-γ (*rIFN-γ*) (n = 4). One-way ANOVA with Holm-Sidak's multiple comparisons *post hoc* test. **D,** Flow cytometry of PD-L1 expression on $V\delta1^+CD103^+$ cells from human gut after overnight culture with media alone or human rIFN-γ. Data obtained from 3 independent donors. $*P < .05$, $**P < .01$,$***P < .001$.

Our findings evoke seminal studies of Pace et al[76] who showed that a key consequence of T_{reg} activity in *Listeria* infection was to limit memory compartments to higher affinity, more efficacious, antibacterial T cells that were less susceptible to control by T_{reg} cells. In this light, it is also the case that the perpetuation of T_{RM} cells that show low-affinity cross-reactivity toward neoantigens, for example, T_{RM} cells induced by common cold coronaviruses that have low affinity for severe acute respiratory syndrome coronavirus 2 antigens, may contribute to immunopathology[77] and may offer another rationale for locally regulating T_{RM}-cell quality.

Note however that this consideration does not dismiss the prospect that some T cells bearing lower affinity TCRs may form T_{RM} cells whose cross-reactivity provides valuable contributions to a first line of defense.[42,78] Such contributions might be more important at later time points when the immediate prospects of re-encountering the initial challenge have declined, and when the regulatory influence of DETCs will presumably be reduced by their evident spatial exclusion.[7]

T_{RM}-cell infiltration and quality has been shown by independent approaches to be a better prognostic marker of cancer suppression than was the quantification of circulating $CD8^+$ T cells,[79-81] highlighting the importance of markers of T_{RM}-cell quality. In that regard, our studies suggest that CD5 may be a useful discriminator of the quality of the T_{RM}-cell compartment, as may be RANKL. At the same time, T_{RM} cells can mediate allergic immunopathologies, as in ACD, and may also mediate severe adverse events during the clinical blockade of PD1 and/or other immunological checkpoints in patients with cancer. Our study raises the interesting possibility that in all these settings, the multipartite, ecological nature of local immune responses may frequently reflect critical integrations of lymphocytes of distinct lineages that are most often studied entirely separately. Indeed, at least some of the contributions of γδ T cells to cancer control[13,82] might in part reflect their impact on T_{RM} cells rather than their direct targeting of malignant cells. Likewise, anatomical site-specific variations in the responsiveness and effector potentials of T_{RM} cells may map back to variations in tissue-intrinsic innate-like lymphocytes at steady-state and in their responsiveness to local changes in tissue status, which in the case studied here was ACD. This could have profound clinical implications and would seem an important area to pursue. Indeed, one might consider that enhancing local ecological regulation by tissue-intrinsic lymphocytes might ameliorate some examples of organ-specific allergic and/or autoimmune disease.

DISCLOSURE STATEMENT

Supported by the Francis Crick Institute, which receives core funding from Cancer Research UK (CRUK); the UK Medical Research Council; the Wellcome Trust (FC001003); the CRUK King's Cancer Centre; the National Institute for Health and Care research Biomedical Research Center at Guy's and St Thomas' National Health Service Foundation Trust and King's College London; and the European Molecular Biology Organization (ALTF 198–2018 to M.M.R.). Y.W. is supported by a Wellcome Trust Clinical Research Career Development Fellowship (220589/Z/20/Z). M.L.I. and D.D. were supported in part by Gamma Delta Therapeutics. The funders had no role in study design, data collection and analysis, decision to publish, or preparation of the manuscript.

Disclosure of potential conflict of interest: A.C. Hayday is cofounder and equity holder in ImmunoQure AG; receives research support from Takeda Pharmaceuticals, the Wellcome Trust, the Medical Research Council, and Cancer Research UK; and is a consultant for Takeda Pharmaceuticals, Prokarium, ImmunoQure, and TransImmune AG. Y.W. consults for PersonGen BioTherapeutics Ltd. The rest of the authors declare that they have no relevant conflicts of interest.

We thank the Immunosurveillance Laboratory members, particularly L. Monin, F. Cano, A. Laing, S. Kamdar, and N. Roberts for advice and discussions; A. Baulies (Francis Crick Institute) for data analysis; P. Vantourout for advice and providing PBMC samples; S. Mensurado for sharing protocols; and B. Silva-Santos and F. Di Rosa for discussions.

Key messages

- **Profound regulation of tissue-infiltrating $CD8^+$ αβ T cells by local γδ T cells.**
- **Local γδ T cells sense IFN-γ produced by tissue-infiltrating CD8 T cells establishing a coregulatory axis involving PD-L1 that seems conserved in humans.**
- **PD-L1 blockade may promote CD8 T-effector cell function at the cost of memory T-cell quality.**

REFERENCES

1. Masopust D, Soerens AG. Tissue-resident T cells and other resident leukocytes. Annu Rev Immunol 2019;37:521-46.
2. Schenkel JM, Masopust D. Tissue-resident memory T cells. Immunity 2014;41:886-97.
3. Chorro L, Sarde A, Li M, Woollard KJ, Chambon P, Malissen B, et al. Langerhans cell (LC) proliferation mediates neonatal development, homeostasis, and inflammation-associated expansion of the epidermal LC network. J Exp Med 2009;206:3089-100.
4. Ikuta K, Kina T, MacNeil I, Uchida N, Peault B, Chien YH, et al. A developmental switch in thymic lymphocyte maturation potential occurs at the level of hematopoietic stem cells. Cell 1990;62:863-74.
5. Lewis JM, Girardi M, Roberts SJ, Barbee SD, Hayday AC, Tigelaar RE. Selection of the cutaneous intraepithelial gammadelta+ T cell repertoire by a thymic stromal determinant. Nat Immunol 2006;7:843-50.
6. Park S, Matte-Martone C, Gonzalez DG, Lathrop EA, May DP, Pineda CM, et al. Skin-resident immune cells actively coordinate their distribution with epidermal cells during homeostasis. Nat Cell Biol 2021;23:476-84.
7. Zaid A, Mackay LK, Rahimpour A, Braun A, Veldhoen M, Carbone FR, et al. Persistence of skin-resident memory T cells within an epidermal niche. Proc Natl Acad Sci USA 2014;111:5307-12.
8. Shiohara T, Moriya N, Hayakawa J, Itohara S, Ishikawa H. Resistance to cutaneous graft-vs.-host disease is not induced in T cell receptor delta gene-mutant mice. J Exp Med 1996;183:1483-9.
9. Girardi M, Lewis J, Glusac E, Filler RB, Geng L, Hayday AC, et al. Resident skin-specific gammadelta T cells provide local, nonredundant regulation of cutaneous inflammation. J Exp Med 2002;195:855-67.
10. Chen Y, Chou K, Fuchs E, Havran WL, Boismenu R. Protection of the intestinal mucosa by intraepithelial gamma delta T cells. Proc Natl Acad Sci USA 2002;99:14338-43.
11. Hayday A, Tigelaar R. Immunoregulation in the tissues by gammadelta T cells. Nat Rev Immunol 2003;3:233-42.
12. Mukasa A, Hiromatsu K, Matsuzaki G, O'Brien R, Born W, Nomoto K. Bacterial infection of the testis leading to autoaggressive immunity triggers apparently opposed responses of alpha beta and gamma delta T cells. J Immunol 1995;155:2047-56.
13. Girardi M, Oppenheim DE, Steele CR, Lewis JM, Glusac E, Filler R, et al. Regulation of cutaneous malignancy by gammadelta T cells. Science 2001;294:605-9.
14. Jameson JM, Cauvi G, Witherden DA, Havran WL. A keratinocyte-responsive gamma delta TCR is necessary for dendritic epidermal T cell activation by

damaged keratinocytes and maintenance in the epidermis. J Immunol 2004;172:3573-9.
15. Strid J, Roberts SJ, Filler RB, Lewis JM, Kwong BY, Schpero W, et al. Acute upregulation of an NKG2D ligand promotes rapid reorganization of a local immune compartment with pleiotropic effects on carcinogenesis. Nat Immunol 2008;9:146-54.
16. Witherden DA, Verdino P, Rieder SE, Garijo O, Mills RE, Teyton L, et al. The junctional adhesion molecule JAML is a costimulatory receptor for epithelial gammadelta T cell activation. Science 2010;329:1205-10.
17. McKenzie DR, Hart R, Bah N, Ushakov DS, Muñoz-Ruiz M, Feederle R, et al. Normality sensing licenses local T cells for innate-like tissue surveillance. Nat Immunol 2022;23:411-22.
18. Vocanson M, Hennino A, Cluzel-Tailhardat M, Saint-Mezard P, Benetiere J, Chavagnac C, et al. CD8+ T cells are effector cells of contact dermatitis to common skin allergens in mice. J Invest Dermatol 2006;126:815-20.
19. Demehri S, Cunningham TJ, Hurst EA, Schaffer A, Sheinbein DM, Yokoyama WM. Chronic allergic contact dermatitis promotes skin cancer. J Clin Invest 2014;124:5037-41.
20. Miyake T, Egawa G, Chow Z, Asahina R, Otsuka M, Nakajima S, et al. Circadian rhythm affects the magnitude of contact hypersensitivity response in mice. Allergy 2022;77:2748-59.
21. Mackay LK, Stock AT, Ma JZ, Jones CM, Kent SJ, Mueller SN, et al. Long-lived epithelial immunity by tissue-resident memory T (TRM) cells in the absence of persisting local antigen presentation. Proc Natl Acad Sci USA 2012;109:7037-42.
22. Fulton RB, Hamilton SE, Xing Y, Best JA, Goldrath AW, Hogquist KA, et al. The TCR's sensitivity to self peptide-MHC dictates the ability of I CD8(+) T cells to respond to foreign antigens. Nat Immunol 2015;16:107-17.
23. Mandl JN, Monteiro JP, Vrisekoop N, Germain RN. T cell-positive selection uses self-ligand binding strength to optimize repertoire recognition of foreign antigens. Immunity 2013;38:263-74.
24. Persaud SP, Parker CR, Lo W-L, Weber KS, Allen PM. Intrinsic CD4+ T cell sensitivity and response to a pathogen are set and sustained by avidity for thymic and peripheral complexes of self peptide and MHC. Nat Immunol 2014;15:266-74.
25. Lee H-M, Fleige A, Forman R, Cho S, Khan AA, Lin L-L, et al. IFNγ signaling endows DCs with the capacity to control type I inflammation during parasitic infection through promoting T-bet+ regulatory T cells. PLoS Pathog 2015;11:e1004635.
26. Stetson DB, Mohrs M, Reinhardt RL, Baron JL, Wang Z-E, Gapin L, et al. Constitutive cytokine mRNAs mark natural killer (NK) and NK T cells poised for rapid effector function. J Exp Med 2003;198:1069-76.
27. Moran AE, Holzapfel KL, Xing Y, Cunningham NR, Maltzman JS, Punt J, et al. T cell receptor signal strength in Treg and iNKT cell development demonstrated by a novel fluorescent reporter mouse. J Exp Med 2011;208:1279-89.
28. Huang S, Hendriks W, Althage A, Hemmi S, Bluethmann H, Kamijo R, et al. Immune response in mice that lack the interferon-gamma receptor. Science 1993;259:1742-5.
29. Zhang B, Wu J, Jiao Y, Bock C, Dai M, Chen B, et al. Differential requirements of TCR signaling in homeostatic maintenance and function of dendritic epidermal T cells. J Immunol 2015;195:4282-91.
30. Clark RA, Chong B, Mirchandani N, Brinster NK, Yamanaka K-I, Dowgiert RK, et al. The vast majority of CLA+ T cells are resident in normal skin. J Immunol 2006;176:4431-9.
31. Jamal-Hanjani M, Wilson GA, McGranahan N, Birkbak NJ, Watkins TBK, Veeriah S, et al. Tracking the evolution of non-small-cell lung cancer. N Engl J Med 2017;376:2109-21.
32. Mallick-Wood CA, Lewis JM, Richie LI, Owen MJ, Tigelaar RE, Hayday AC. Conservation of T cell receptor conformation in epidermal gammadelta cells with disrupted primary Vgamma gene usage. Science 1998;279:1729-33.
33. Bolger AM, Lohse M, Usadel B. Trimmomatic: a flexible trimmer for Illumina sequence data. Bioinformatics 2014;30:2114-20.
34. Dobin A, Davis CA, Schlesinger F, Drenkow J, Zaleski C, Jha S, et al. STAR: ultrafast universal RNA-seq aligner. Bioinformatics 2013;29:15-21.
35. Li B, Dewey CN. RSEM: accurate transcript quantification from RNA-Seq data with or without a reference genome. BMC Bioinformatics 2011;12:323.
36. Love MI, Huber W, Anders S. Moderated estimation of fold change and dispersion for RNA-seq data with DESeq2. Genome Biol 2014;15:550.
37. Butler A, Hoffman P, Smibert P, Papalexi E, Satija R. Integrating single-cell transcriptomic data across different conditions, technologies, and species. Nat Biotechnol 2018;36:411-20.
38. Schindelin J, Arganda-Carreras I, Frise E, Kaynig V, Longair M, Pietzsch T, et al. Fiji: an open-source platform for biological-image analysis. Nat Methods 2012;9:676-82.
39. Kok L, Dijkgraaf FE, Urbanus J, Bresser K, Vredevoogd DW, Cardoso RF, et al. A committed tissue-resident memory T cell precursor within the circulating CD8+ effector T cell pool. J Exp Med 2020;217:e20191711.
40. Clarke J, Panwar B, Madrigal A, Singh D, Gujar R, Wood O, et al. Single-cell transcriptomic analysis of tissue-resident memory T cells in human lung cancer. J Exp Med 2019;216:2128-49.
41. Park SL, Zaid A, Hor JL, Christo SN, Prier JE, Davies B, et al. Local proliferation maintains a stable pool of tissue-resident memory T cells after antiviral recall responses. Nat Immunol 2018;19:183-91.
42. Fiege JK, Stone IA, Fay EJ, Markman MW, Wijeyesinghe S, Macchietto MG, et al. The impact of TCR signal strength on resident memory T cell formation during influenza virus infection. J Immunol 2019;203:936-45.
43. Boddupalli CS, Nair S, Gray SM, Nowyhed HN, Verma R, Gibson JA, et al. ABC transporters and NR4A1 identify a quiescent subset of tissue-resident memory T cells. J Clin Invest 2016;126:3905-16.
44. Wang R, Zhang L, Zhang X, Moreno J, Celluzzi C, Tondravi M, et al. Regulation of activation-induced receptor activator of NF-kappaB ligand (RANKL) expression in T cells. Eur J Immunol 2002;32:1090-8.
45. Barbee SD, Woodward MJ, Turchinovich G, Mention J-J, Lewis JM, Boyden LM, et al. Skint-1 is a highly specific, unique selecting component for epidermal T cells. Proc Natl Acad Sci USA 2011;108:3330-5.
46. Girardi M, Oppenheim D, Glusac EJ, Filler R, Balmain A, Tigelaar RE, et al. Characterizing the protective component of the alphabeta T cell response to transplantable squamous cell carcinoma. J Invest Dermatol 2004;122:699-706.
47. Stuart T, Butler A, Hoffman P, Hafemeister C, Papalexi E, Mauck WM, et al. Comprehensive integration of single-cell data. Cell 2019;177:1888-902.e21.
48. Mackay LK, Rahimpour A, Ma JZ, Collins N, Stock AT, Hafon M-L, et al. The developmental pathway for CD103(+)CD8+ tissue-resident memory T cells of skin. Nat Immunol 2013;14:1294-301.
49. Kumar BV, Ma W, Miron M, Granot T, Guyer RS, Carpenter DJ, et al. Human tissue-resident memory T cells are defined by core transcriptional and functional signatures in lymphoid and mucosal sites. Cell Rep 2017;20:2921-34.
50. Savas P, Virassamy B, Ye C, Salim A, Mintoff CP, Caramia F, et al. Single-cell profiling of breast cancer T cells reveals a tissue-resident memory subset associated with improved prognosis. Nat Med 2018;24:986-93.
51. Cho J-H, Kim H-O, Ju Y-J, Kye Y-C, Lee G-W, Lee S-W, et al. CD45-mediated control of TCR tuning in naïve and memory CD8+ T cells. Nat Commun 2016;7:13373.
52. Dong S, Corre B, Foulon E, Dufour E, Veillette A, Acuto O, et al. T cell receptor for antigen induces linker for activation of T cell-dependent activation of a negative signaling complex involving Dok-2, SHIP-1, and Grb-2. J Exp Med 2006;203:2509-18.
53. Voisinne G, Gonzalez de Peredo A, Roncagalli R. CD5, an undercover regulator of TCR signaling. Front Immunol 2018;9:2900.
54. Jiang X, Park CO, Geddes Sweeney J, Yoo MJ, Gaide O, Kupper TS. Dermal γδ T cells do not freely re-circulate out of skin and produce IL-17 to promote neutrophil infiltration during primary contact hypersensitivity. PLoS One 2017;12:e0169397.
55. Krause CD, Mei E, Xie J, Jia Y, Bopp MA, Hochstrasser RM, et al. Seeing the light: preassembly and ligand-induced changes of the interferon gamma receptor complex in cells. Mol Cell Proteomics 2002;1:805-15.
56. Ma X, Ling KW, Dzierzak E. Cloning of the Ly-6A (Sca-1) gene locus and identification of a 3' distal fragment responsible for high-level gamma-interferon-induced expression in vitro. Br J Haematol 2001;114:724-30.
57. Krummel MF, Mahale JN, Uhl LFK, Hardison EA, Mujal AM, Mazet JM, et al. Paracrine costimulation of IFN-γ signaling by integrins modulates CD8 T cell differentiation. Proc Natl Acad Sci USA 2018;115:11585-90.
58. Schenkel JM, Fraser KA, Vezys V, Masopust D. Sensing and alarm function of resident memory CD8+ T cells. Nat Immunol 2013;14:509-13.
59. Hirano T, Honda T, Kanameishi S, Honda Y, Egawa G, Kitoh A, et al. PD-L1 on mast cells suppresses effector CD8+ T-cell activation in the skin in murine contact hypersensitivity. J Allergy Clin Immunol 2021;148:563-73.e7.
60. Fife BT, Pauken KE, Eagar TN, Obu T, Wu J, Tang Q, et al. Interactions between PD-1 and PD-L1 promote tolerance by blocking the TCR-induced stop signal. Nat Immunol 2009;10:1185-92.
61. Kortlever RM, Sodir NM, Wilson CH, Burkhart DL, Pellegrinet L, Brown Swigart L, et al. Myc cooperates with Ras by programming inflammation and immune suppression. Cell 2017;171:1301-15.e14.
62. Herndler-Brandstetter D, Ishigame H, Shinnakasu R, Plajer V, Stecher C, Zhao J, et al. KLRG1+ effector CD8+ T cells lose KLRG1, differentiate into all memory T cell lineages, and convey enhanced protective immunity. Immunity 2018;48:716-29.e8.
63. Johnson MD, Otuki MF, Cabrini DA, Rudolph R, Witherden DA, Havran WL. Hspa8 and ICAM-1 as damage-induced mediators of γδ T cell activation. J Leukoc Biol 2021;111:135-45.
64. Fujita M, Miyachi Y, Nakata K, Imamura S. Gamma delta T-cell receptor-positive cells of human skin: II. Appearance in delayed-type hypersensitivity reaction. Arch Dermatol Res 1993;285:436-40.

65. Czarnowicki T, Santamaria-Babí LF, Guttman-Yassky E. Circulating CLA+ T cells in atopic dermatitis and their possible role as peripheral biomarkers. Allergy 2017; 72:366-72.
66. Le Floc'h A, Jalil A, Vergnon I, Le Maux Chansac B, Lazar V, Bismuth G, et al. Alpha E beta 7 integrin interaction with E-cadherin promotes antitumor CTL activity by triggering lytic granule polarization and exocytosis. J Exp Med 2007;204:559-70.
67. Schenkel JM, Fraser KA, Beura LK, Pauken KE, Vezys V, Masopust D. T cell memory: resident memory CD8 T cells trigger protective innate and adaptive immune responses. Science 2014;346:98-101.
68. Hirai T, Zenke Y, Yang Y, Bartholin L, Beura LK, Masopust D, et al. Keratinocyte-mediated activation of the cytokine TGF-β maintains skin recirculating memory CD8+ T cells. Immunity 2019;50:1249-61.e5.
69. Ferreira C, Barros L, Baptista M, Blankenhaus B, Barros A, Figueiredo-Campos P, et al. Type 1 Treg cells promote the generation of CD8+ tissue-resident memory T cells. Nat Immunol 2020;21:766-76.
70. Spidale NA, Malhotra N, Frascoli M, Sylvia K, Miu B, Freeman C, et al. Neonatal-derived IL-17 producing dermal γδ T cells are required to prevent spontaneous atopic dermatitis. eLife 2020;9:e51188.
71. Fan X, Rudensky AY. Hallmarks of tissue-resident lymphocytes. Cell 2016;164: 1198-211.
72. Hayday AC. γδ T cell update: adaptate orchestrators of immune surveillance. J Immunol 2019;203:311-20.
73. Pauken KE, Godec J, Odorizzi PM, Brown KE, Yates KB, Ngiow SF, et al. The PD-1 pathway regulates development and function of memory CD8+ T cells following respiratory viral infection. Cell Rep 2020;31:107827.
74. Wyss L, Stadinski BD, King CG, Schallenberg S, McCarthy NI, Lee JY, et al. Affinity for self antigen selects Treg cells with distinct functional properties. Nat Immunol 2016;17:1093-101.
75. Cho J-H, Sprent J. TCR tuning of T cell subsets. Immunol Rev 2018;283:129-37.
76. Pace L, Tempez A, Arnold-Schrauf C, Lemaitre F, Bousso P, Fetler L, et al. Regulatory T cells increase the avidity of primary CD8+ T cell responses and promote memory. Science 2012;338:532-6.
77. Bacher P, Rosati E, Esser D, Martini GR, Saggau C, Schiminsky E, et al. Low-avidity CD4+ T cell responses to SARS-CoV-2 in unexposed individuals and humans with severe COVID-19. Immunity 2020;53(6):1258-71.e5.
78. Lipsitch M, Grad YH, Sette A, Crotty S. Cross-reactive memory T cells and herd immunity to SARS-CoV-2. Nat Rev Immunol 2020;20:709-13.
79. Ganesan A-P, Clarke J, Wood O, Garrido-Martin EM, Chee SJ, Mellows T, et al. Tissue-resident memory features are linked to the magnitude of cytotoxic T cell responses in human lung cancer. Nat Immunol 2017;18:940-50.
80. Nizard M, Roussel H, Diniz MO, Karaki S, Tran T, Voron T, et al. Induction of resident memory T cells enhances the efficacy of cancer vaccine. Nat Commun 2017;8:15221.
81. Milner JJ, Toma C, Yu B, Zhang K, Omilusik K, Phan AT, et al. Runx3 programs CD8+ T cell residency in non-lymphoid tissues and tumours. Nature 2017;552: 253-7.
82. Liu Z, Eltoum I-EA, Guo B, Beck BH, Cloud GA, Lopez RD. Protective immunosurveillance and therapeutic antitumor activity of gammadelta T cells demonstrated in a mouse model of prostate cancer. J Immunol 2008;180: 6044-53.